A hydrogeological conceptual model of aquifers in catchments headed by temperate glaciers

Aude Vincent[1, 2], Clémence Daigre[2], Ophélie Fischer[2], Guðfinna Aðalgeirsdóttir[1], Sophie Violette[2, 3], Jane Hart[4], Snævarr Guðmundsson[5], Finnur Pálsson[1]

[1]~~Glaciology Team,~~ Institute of Earth Sciences, University of Iceland, Askja, Sturlugata 7, IS-101 Reykjavík, Iceland
[2]Geology Laboratory, École Normale Supérieure - PSL & CNRS, UMR.8538, 24 rue Lhomond, 75231, Paris Cedex, France
[3]UFR.918, Sorbonne University, 4, Place Jussieu, 75252, Paris Cedex, France
[4]Geography and Environmental Science, University of Southampton, Southampton SO17 1BJ, UK
[5]South East Iceland Nature Research Center, Nýheimar, Litlubrú 2, IS-780 Höfn í Hornafirði, Iceland

Correspondence to: Aude Vincent (aude.vincent@normalesup.org)

Abstract. Achieving understanding and quantification of unknown aquifer systems in glacial context is crucial to forecast the evolution under climate change of water resources and of potential floods and landslide~~s~~ hazards. We focus on four south-eastern outlet glaciers of the largest~~main~~ Icelandic icecap, Vatnajökull. New data are ~~being~~ acquired in the field to characterise groundwater dynamics. From th ese data~~is~~ we propose a hydrogeological conceptual model: two distinct aquifers and their hydraulic conductivities are identified. A comprehensive water balance at the scale of the watershed is ~~has been~~ obtained. Recharge to the aquifers is up to 4 times higher under the glaciers than on the plain, and we demonstrate the glacial melt recharge impact on the groundwater dynamic.

Keywords. groundwater; glacier; recharge rate; hydraulic conductivity; data acquisition; climate change; Iceland

1 Introduction

The research addressing glacier evolution under climate change is well developed, looking not only at changes in mass balance (e.g.: Aðalgeirsdóttir et al., 2020; Björnsson et al., 2013; ~~Gardner et al 2013;~~ Jóhannesson et al., 2020; Rounce et al., 2023), but also at the associated effects on basal and downstream hydrology (e.g. Immerzeel~~Li~~ et al., 2020~~15~~). However, aftermath changes to the groundwater component are rarely considered (Vincent et al., 2019), though evolving groundwater recharge, discharge and storage in glacierised catchments is required to forecast the future changes in water resources and of water-related hazards (landslides, floods) under climate change.

Available studies in similar glacierised catchments show: high recharge to aquifers by glacial meltwater (Mackay et al., 2020; Sigurðsson, 1990), and strong connection between surface water and groundwater (e.g. Dochartaigh et al., 2019; ~~Somers et al., 2016;~~ see Vincent et al., 2019 for other references). Such studies are few and data relate only to shallow and unconfined aquifers (Dochartaigh et al., 2019; Mackay et al., 2020).

This study is focusing on four outlet glaciers at the south-east margin of Vatnajökull, Iceland's largest icecap. The total volume of glaciers in Iceland is ~3500 km^3, storing about 20 years of precipitation (Björnsson and Pálsson, 2008). The studied outlet glaciers, Fláajökull, Heinabergsjökull, Skálafellsjökull and Breiðamerkurjökull, like all glaciers in Iceland are temperate and warm based. They have been retreating since the mid-1990s due to climate change (e.g. Aðalgeirsdóttir et al., 2020; Björnsson et al., 2013). The 4 outlet glaciers' catchments cover 1300 km^2 (fig. 1). The geology is mainly composed of basalt, till and glacio-fluvial deposits (Jóhannesson and Sæmundsson, 1998).

Our goal is to understand and characterise the whole hydrogeological system, including its recharge, its geometry and the hydraulic parameters of the aquifers. In particular questions that are lacking answers in the current state of the art: i) Does meltwater from the glacier recharge the aquifer(s) beneath the ice, (ii) How much water from the glacier melt does this represent? (iii) Is there only one aquifer in the superficial geological formation or also one in the bedrock?

To answer these questions we are: (i) Acquiring new data since May 2021 on groundwater level, temperature and electro-conductivity (EC) in an observation network of 18 boreholes including 4 newly drilled ones; (ii) Analysing existing and newly acquired data to obtain the extent and thickness of the geological formations (from geological and drilling data), the recharge rates (from existing data: glacier mass balance and weather data) and hydraulic parameters (from existing grain size data, new slug tests and new groundwater level data). Finally, we provide a hydrogeological conceptual model of the system based on all the data.
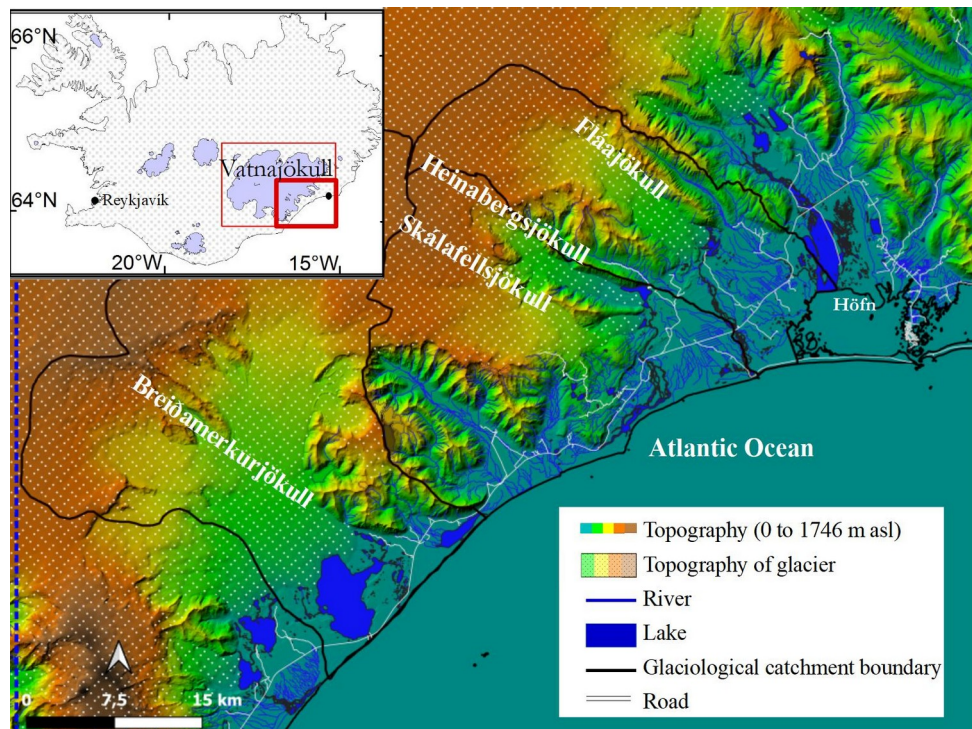

Figure 1: Situation map of the study area showing topography of the plains and top of the glaciers (IslandsDEMv1, Landmælingar Íslands), glaciological catchments boundaries of the four studied outlet glaciers, river network and lakes (contours Landmælingar Íslands ISN2016). Insert map on the top left corner shows the location of the study area in Iceland, points indicate locations of Reykjavík and Höfn.

Our goals are the following: i) proving whether or not meltwater from the glacier recharges the aquifer(s) beneath the ice sheet, and (ii) how much water from the glacier melt does this represent. To answer these questions we are: (i) Acquiring new data since May 2021 on groundwater level, temperature and electro-conductivity (EC) in an observation network of 18 boreholes including 4 newly drilled ones; (ii) Analysing existing and newly acquired data to obtain the extent and thickness of the geological formations (from geological and drilling data), the recharge rates (from existing data: glacier mass balance and weather data) and hydraulic parameters (from existing grain size data, new slug tests and new groundwater level data). Finally, we provide a hydrogeological conceptual model of the system based on all the data.
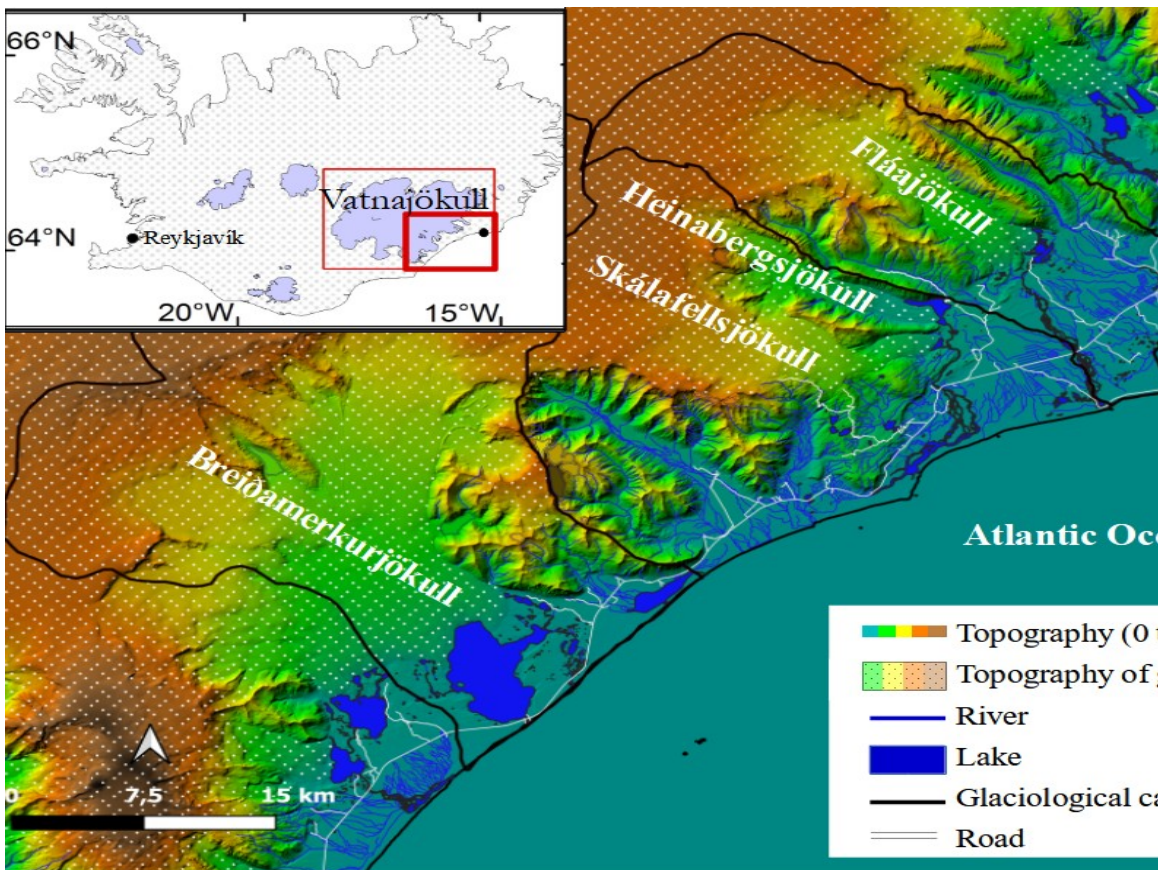
2 Study Area

Iceland's climate is subpolar oceanic, strongly moderated by the Gulf Stream influence (Irminger current) to the south (Björnsson, 2017; Van Vliet-Lanoë et al., 2021). Snow is abundant during winter, especially over 400 m a.s.l. (above sea level) (Van Vliet-Lanoë et al., 2021) and precipitation increase with elevation (Crochet et al., 2007).

Meteorological data are provided by the Icelandic Meteorological Office (IMO). In particular air temperature (T) and precipitation (P) data are recorded at four weather stations closed to Höfn í Hornafirði since June 1965 (fig. 2). The four stations are very close to each other (fig. 3). There is never the same period recorded, except for T between 2007 and 2018 (stations 705 and 5544, fig. 2), with very similar data (correlation coefficient of 0.998). Thus we consider that we can merge the time series of the four stations. A daily record of both temperature and precipitation is obtained from June 1965 to September 2022, with only four months missing (September to December 2006).
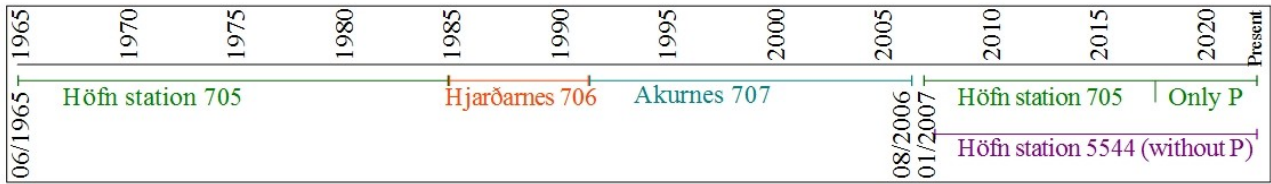
3

Figure 2: Time periods of monitoring of Höfn weather stations: Höfn 705, Höfn 5544, Hjarðarnes 706 and Akurnes 707. Location of the four stations <u>is shown</u> **on fig. 3.**
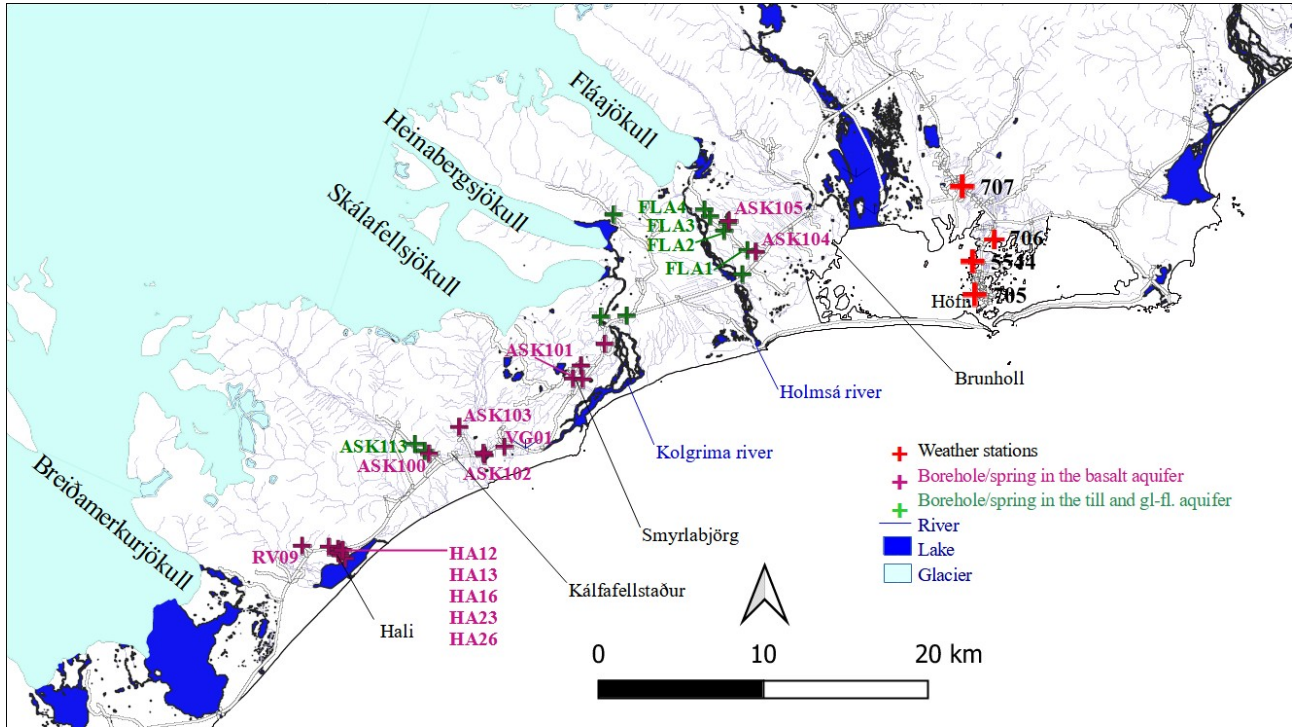

<u>Figure 3: Map of the groundwater observation network, Purple crosses: boreholes and springs in the basalt aquifer, Green crosses: boreholes and springs in the till and glacio-fluvial deposits aquifer (gl. fl.), with location of Höfn weather stations (red crosses): Höfn 705 (+4 m a.s.l.), Höfn 5544 (+5 m a.s.l.), Hjarðarnes 706 (+9 m a.s.l.) and Akurnes 707 (+17 m a.s.l.). Contours are from Landmælingar Íslands ISN2016.</u>
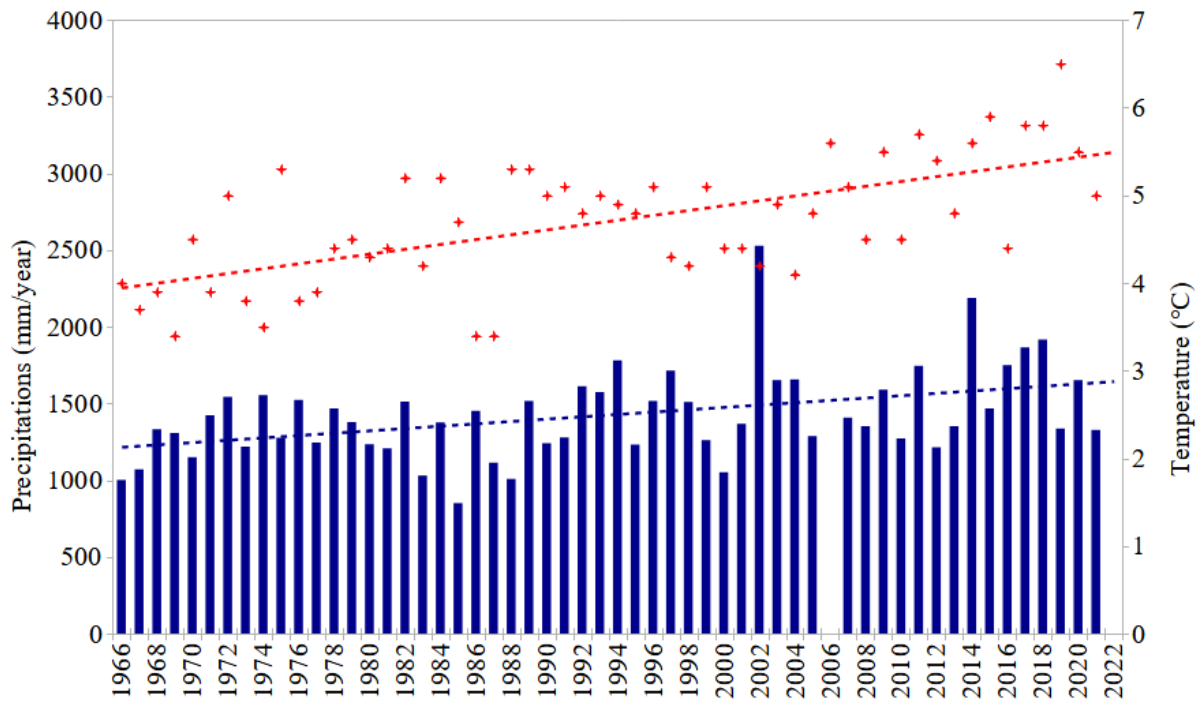
<u>The meteorological data available show that between 1966 to 2021: the annual average temperature has increased from 3.9 to 5.4 °C (+ 1.5 °C, fig. 4), and the annual total precipitation has increased from 1200 to 1630 mm (+ 430 mm, fig. 4). For comparison, the global temperature has increased by + 1.08 ± 0.13 °C between 1850–1900 and 2021 (WMO, 2021). For the studied area, the annual average temperature and total precipitation in 2021 (5 °C and 1327 mm) lies in the 40 % warmest and is in the 40 % driest years (fig. 4). The mean monthly temperatures are distributed on a quite narrow range (fig. 5a), and nearly always stay positive, which is typical for a subpolar oceanic climate. All months receive significant precipitation, but the variation between years is high (fig. 5b).</u>

Figure 4: Weather variables recorded in Höfn from 1966 to 2021 (combined record of 4 stations): Annual average temperature (red crosses, interannual mean over the whole period: 4.7°C) and Annual total precipitation (blue histograms, interannual mean over the whole period: 1420 mm), with linear trends (dot lines: red for temperatures and blue for precipitations).
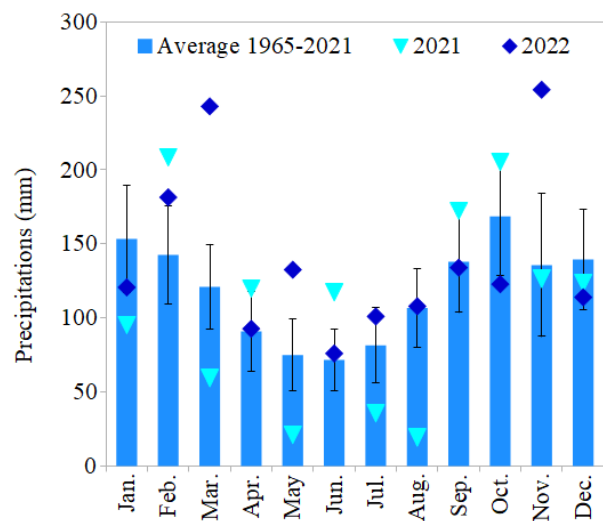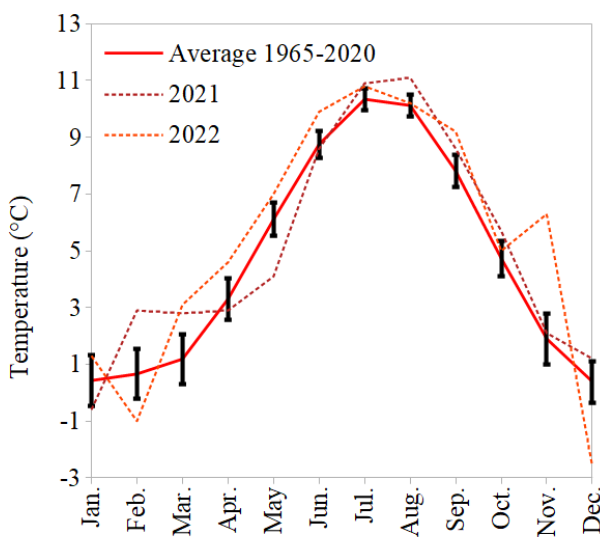
■ Precipitations
+ Temperature

Figure 5: Monthly average of mean temperatures and of precipitation measured in Höfn from 1966 to 2020 (combined record of 4 stations), with monthly standard deviation, and 2021 and 2022 values: a) Temperatures (monthly standard deviation from 0.7 °C to 1.8 °C); b) Precipitation (monthly standard deviation from 41 to 98 mm).

120 The studied glaciers have undergone a complex evolution since their last maximum of extension at the end of the 19th century (Hannesdóttir et al., 2015). There retreat since the mid 1990s (Björnsson et al., 2013) is linked to climate change (e.g. Aðalgeirsdóttir et al., 2020). It has slowed down since 2010 and its variability increased (Noël et al., 2022) highlightning the high sensitivity of glaciers to climate and oceanic factors. The retreat rate is predicted to increase again after 2050 (Noël et al., 2022). Breiðamerkurjökull has a particularly quick retreat rate because of its unique

125 situation, with its proglacial lake in direct and close connection with the ocean, the heat exchange with the ocean through tidal currents enhancing the melting rate (Guðmundsson et al., 2020). Data on the mass balance of the glaciers (here only summer mass balance) are extrapolated from stake measurements (glaciological method, Cogley et al., 2011) on the Vatnajökull (Björnsson et al., 1998; Björnsson et al., 2013; Pálsson et al., 2022) in the period 1992/93–2021.

The studied glaciers are temperate and warm based. They have undergone a complex evolution since their last

130 maximum of extension at the end of the 19th century (Hannesdóttir et al., 2015). There recession since the mid 1990s (Björnsson et al., 2013) is linked to climate change (e.g. Aðalgeirsdóttir et al., 2020). It has slowed down since 2010 (Noël et al., 2022), underlying the high sensitivity of glaciers to climate and oceanic factors. The retreat rate is predicted to increase again in the next decades (Noël et al., 2022). Breiðamerkurjökull has a particularly quick retreat rate because of its unique situation, with its proglacial lake in direct and close communication with the ocean, which currents are

135 enhancing the melting rate (Guðmundsson et al., 2020). Data on the mass balance of the glaciers (here only summer mass balance) are extrapolated from stake measurements (glaciological method, Cogley et al., 2011) on the Vatnajökull (Björnsson et al., 1998; Björnsson et al., 2013; Pálsson et al., 2022) in the period 1992/93–2021.

The studied se glaciers are lying on volcanic rocks (Einarsson, 1994) and volcano-detritic deposits. The interaction of a rift zone, the Mid-Atlantic Ridge, and a mantle plume, the Iceland Mantle Plume, has formed the Iceland Plateau

140 (Martin et al., 2011; Sæmundsson, 1979). Four main groups of geological formations exist (Einarsson, 1994), of those 2 are represented in the study area: Tertiary Basalt formations and sediments. The basalt encountered in the study area was formed during the Miocene and Pliocene (-13 Ma in the east of Iceland to -3.3 Ma for the west margin of Vatnajökull, (Torfason, 1979)). This pile, of a total thickness up to 12 km (Torfason 1979), and gently inclined towards the north-west (Torfason, 1979), is mainly composed of basaltic lava flows, with numerous acidic intrusions and

145 intercalated sediments which have been largely eroded (Jóhannesson and Sæmundsson, 1998). Indeed the Vatnajökull outlet glaciers have carved out steep sided valley in the basaltic plateau (Hannesdóttir et al., 2010). In the study area the basaltic plateau toped with the glacier reaches a maximum elevation of 1746 m a.s.l.. (glacier thickness included). Till is the sediment formed, transported and deposited by glaciers movements (Goldthwait, 1971), with little or no sorting by water (Dreimanis, 1983). In the study area, the plains between the glaciers and the coast are sandur (Hannesdóttir et

150 al., 2010), geomorphological features encompassing till and glacio-fluvial deposits. They are partly cultivated (Hannesdóttir et al., 2010). The periglacial landforms are numerous and could induce variation in hydraulic parameters. South of Breiðamerkurjökull in particular there is a large sandur with many drumlins and eskers. The geological map of Iceland at a scale of 1/500 000 was published by the Icelandic Institute of Natural History (Jóhannesson and Sæmundsson, 1998), and is to date the only published geological map covering the study area. The drilling logs of 66

155 boreholes, drilled for different purposes in the past, were collected through the ISOR database (maps.is/os) or directly at the archives of the drilling company Ræktunarsamand Flóa og Skeiða (RFS). Twenty-four of these logs provided

validation for~~allowed to check~~ the geological map and provided data on the formations thicknesses. The type of soil developed in the studied area are Vitric Andosol, Leptosol and Andosols (Arnalds, 1999; Arnalds, 2015).

3 Methodology

The a~~A~~vailable data ~~i~~on the studied area provide information on the geology, the weather and the glaciers evolution, but not on the hydrodynamics. Thus new data acquisition was done before analysing the complete data set.

3.1 New Data Acquisition

Data acquisition in the field has been conducted from May 2021 to September 2022. We have simplified the available geological map (Jóhannesson and Sæmundsson, 1998) to consider the two main geological formations potentially aquiferous~~aquifers~~: the till and glacio-fluvial deposits combined, and the basalt (including the acidic intrusions). We have checked the extent of the outcrops of the till and glacio-fluvial deposits formation and of the basalt formation as indicated on the geological map in the field wherever possible (13 outcrops) and slightly corrected it. The resulting map is presented in fig. 6. We have selected 14 boreholes among the abandoned ones to build the observation network (table 1 and fig. 3), and ~~make~~ drilled 4 additional~~new~~ ones to complete it, downstream of Fláajökull, on a line toward the coast (FLA1, FLA2, FLA3, FLA4). The network thus constitutes of 13 boreholes in the basalt formation and 5 in the till and glacio-fluvial formation. In addition, we monitored 11 depression springs, 4 from the basalt aquifer and 7 from the till and glacio-fluvial deposits aquifer. We made monthly manual measurements from March or May to September of the groundwater level, water temperature and water EC with a manual piezometric probe (Solinst TLC Meter 107). The springs are controlled visually, and their temperature and EC monitored with the TLC Meter. We monitored 4 boreholes in the till and glacio-fluvial deposits and 7 boreholes in the basalt using automatic pressure and temperature probes, at an hourly time step (6 TD-Diver type DI802, 3 TD Micro-Diver type DI501) and 2 probes measuring in addition electro-conductivity (2 CTD-Diver type DI217). To correct for the atmospheric pressure we used 3 Baro Diver type DI800 and 1 Baro Micro-Diver DI500. A participatory approach involving Glacier Adventure, a tourism and educational company based in Hali, allows the monthly monitoring of 3 of the boreholes in the basalt aquifer all year round with an Hydrotechnik Water level meter. All boreholes and springs were localised using a differential GPS in September 2021 (elevations obtained shown in table 1). Finally we carried out slug tests ~~out~~ in July and September 2022 in the 5 boreholes in the till and glacio-fluvial deposits and in 6 boreholes in the basalt formation, using slugs (length 1m, diameters 10 cm and 5 cm) and an automatic pressure probe. One to three repetitions of the test were conducted in each borehole, with data acquired every half second.

Borehole/Spring name	Elevation (m a.s.l.)	Depth (m)	Diameter (m)	Borehole rim height (m)	Year of drilling	Aquifer tapped	Confined /Unconfined
FLA1	8.74 ± 0.04	5.6	0.13	0.15	2021	Till and gl-fl	Unconfined
FLA2	16.49 ± 0.27	6	0.13	0.19	2021	Till and gl-fl	Unconfined
FLA3	24.11 ± 0.25	5.7	0.13	0.36	2021	Till and gl-fl	Unconfined
FLA4	26.02 ± 0.13	5.8	0.13	0.19	2021	Till and gl-fl	Unconfined
ASK113	36.53 ± 0.04	31.5	0.16	0.37	2010	Till and gl-fl	Unconfined
Spring 2 Heinabergsdalur	73.21 ± 0.45	_	_	_	_	Till and gl-fl	Unconfined
R1 near ASK105	19.3 ± 0.5	_	_	_	_	Till and gl-fl	Unconfined

Name	Elevation	Depth	Diameter	Borehole rim height	Year of drilling	Aquifer tapped	Confined/Unconfined
R2 between ASK100 & ASK113	32.5 ± 0.5	_	_	_	_	Till and gl-fl	Unconfined
R5 west of Kolgríma	13.1 ± 0.5	_	_	_	_	Till and gl-fl	Unconfined
R6 west of Hólmsá	8.5 ± 0.5	_	_	_	_	Till and gl-fl	Unconfined
R9 near Brunholl	2.7 ± 0.5	_	_	_	_	Till and gl-fl	Unconfined
ASK100	26.39 ± 0.08	56	0.16		2010	Basalt	Confined
ASK101	37.77 ± 0.08	100	0.16	0.39	2010/2015	Basalt	Confined
ASK102	15.50 ± 0.04	49.6	0.16	0.24	2010	Basalt	Unconfined
ASK103	24.28 ± 0.09	55	0.16	0.31	2010	Basalt	Confined
ASK104	13.59 ± 0.09	50	0.16	0.34	2010	Basalt	Confined
ASK105	20.12 ± 0.21	50	0.16	0.42	2010	Basalt	Unconfined
HA12	54.23 ± 0.06	72	0.16	0.26	2001	Basalt	Confined
HA13	60.80 ± 0.07	49	0.16	0.43	2002	Basalt	Unconfined
HA16	3.14 ± 0.06	54	0.16	0.12	2002	Basalt	Confined
HA23	14.15 ± 0.05	60.5		0.27		Basalt	Confined
HA26	26.20 ± 0.05	70	0.16	0.29	2016	Basalt	Confined
RV09	47.35 ± 0.04	60	0.18	0.44	2016	Basalt	Confined
VG01	11.39 ± 0.3	60		0.34	2002	Basalt	Unconfined
R3 Smyrlabjörg	19.8 ± 0.5	_	_	_	_	Basalt	Unconfined
Spring 1 Smyrlabjörg	15.7 ± 0.5	_	_	_	_	Basalt	Unconfined
R4 near ASK102	6.9 ± 0.5	_	_	_	_	Basalt	Unconfined
R7 Smyrlabjörg – Kolgríma	10.1 ± 0.5	_	_	_	_	Basalt	Unconfined

Table 1: Groundwater observation network description: . For each borehole are detailed their elevation, depth, diameter, borehole rim height, year of drilling, aquifer tapped, and the confined or unconfined status of the tapped aaquifer tapped. For each spring elevation and the aquifer. tapped, are detailed. gl-fl= glacio-fluvial deposits. For location of the rivers and places mentioned see fig. 3.
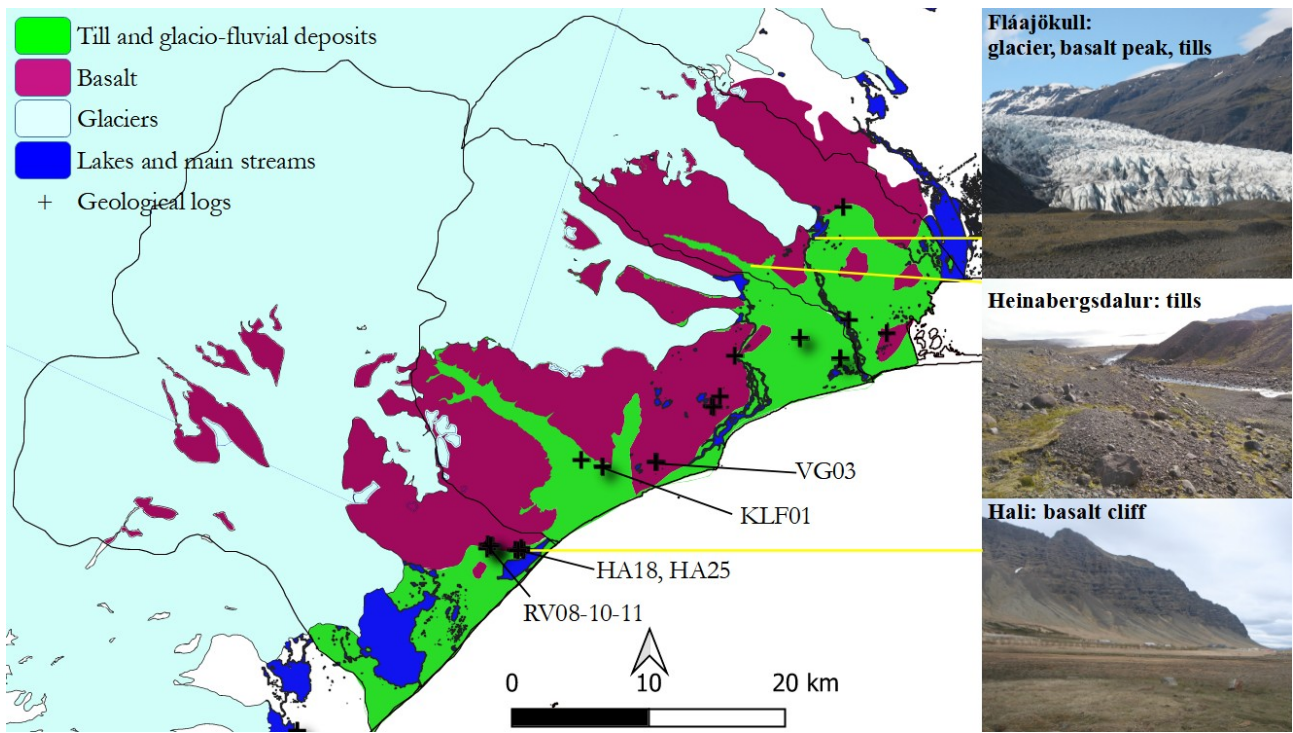
Figure 6: Simplified geological map of the study area, with locations of the geological logs giving information on the geological formations thicknesses. The basalt formation is represented in purple and the till and glacio-fluvial deposits in green. In light blue the glacier, and in dark blue the lakes and main rivers. Pictures on the right side offer some typical views of the geological system: one outlet glacier (Fláajökull), tills in Heinabergsdalur and a basalt cliff at Hali. Geological contours based on Jóhannesson and Sæmundsson 1998; other contours Landmælingar Íslands ISN2016.

3.2 Data Analysis

We used numerous methodologies to analyse the data gathered and acquired; they are listed below.

The potential evapotranspiration (PET) was calculated using Thornthwaite method (Thornthwaite, 1948) for evolution since 1966 and with Penman method (Monteith, 1965; Penman, 1948, with CropWat 8.0) and for monthly values between 1990 and 2022, using available weather data from Höfn weather stations and parameters adjusted to the latitude. We chose classic methods, as from the literature there is no specific method proved more representative for Iceland. Effective rainfall was then calculated, with the following equations:

$if\ P_i > PET_i,$ $RET_i = PET_i$ $and\ if\ S_{i-1} = S_{max}$ $EF_i = P_i - RET_i$,

$otherwise$ $EF_i = P_i - RET_i - (S_{max} - S_{i-1})$

$if\ P_i = PET_i,$ $RET_i = PET_i\ and\ EF_i = 0$

$if\ P_i < PET_i\ and\ P_i + S_i >= PET_i$ $RET_i = PET_i\ and\ EF_i = 0$

$and\ P_i + S_i < PET_i,$ $RET_i = P_i + S_{i-1},\ S_i = S_{i-1} - (PET_i - P_i)\ and\ EF_i = 0$

with $_i$: month; RET_i: Real Evapotranspiration; PET_i: Potential Evapotranspiration; P_i: Precipitation; S_i: Soil water storage capacity, EF_i: Effective Rainfall. S is initially estimated at 50mm, as an average for the Vitric Andosol, Leptosol and Andosols that compose the area (Arnalds, 1999; Arnalds, 2015). As rainfall and snow events are not completely distinguished in the precipitation chronicle provided by the IMO, the effective rainfall we calculate does not represent the delayed recharge to the aquifers due to snow melt.

We used estimates of glacier melt and effective rainfall to deduce the amount of water available for subglacial surface flow and groundwater recharge in the subglacial area. To estimate the glaciers melt, we used two datasets: (i) the estimated summer mass balance based on direct glaciological methods from 2010 to 2021 (Björnsson et al., 1998; Björnsson et al., 2013; Pálsson et al., 2022); and (ii) melt calculated from 1980 to 2016 by Schmidt et al. (2020) running HIRHAM 5 with output from the Regional Climate Model HARMONIE-AROME reanalysis-forced simulations. HARMONIE-AROME is a non-hydrostatic, convection permitting model (Bengtsson et al., 2017), reanalysed by the Icelandic Meteorological Office for Iceland (ICRA) (Nawri et al., 2017), from 1 September 1979 until 31 December 2017, at a horizontal resolution of $0.025° \times 0.025°$, corresponding to ~2.5 km. In the rest of the paper these simulations by Schmidt et al., (2020) are called HIRHAM 5-ICRA. The non-surface mass balance is added to the HIRHAM 5-ICRA outputs: 0.23 mm day^{-1} of dissipation for all the area, and an additional 0.15 mm day^{-1} from lake calving for Breiðamerkurjökull and Heinabergsjökull (Aðalgeirsdóttir et al., 2020; Jóhannesson et al., 2020).

The potential evapotranspiration was calculated using Thornthwaite method (Thornthwaite, 1948) for evolution since 1966 and with Penman method (Monteith, 1965; Penman, 1948, with CropWat 8.0) and for monthly values between 1990 and 2021, using available weather data from Höfn weather stations. Effective rainfall was then calculated, with the following equations:

$if\ P_t + S_t >= PET_t,\ RET_t = PET_t\ and\ if\ P_t < PET_t,\ SW_t = SW_{t-t} - (PET_t - P_t)$

$if\ P_t + S_t < PET_t,\ RET_t = max(P_t + S_t\ ;\ PET_t)\ and\ SW_t = SW_{t-t} - (PET_t - P_t)$

$if\ P_t > RET_t,\ EF_t = P_t - RET_t\ otherwise\ EF_t = 0$

with $_t$: month; RET_t: Real Evapotranspiration; PET_t: Potential EvapoTranspiration; P_t: Precipitation; S_t: Soil water storage capacity, EF_t: Effective Rainfall. SW is initially estimated at 50mm, as an average for the Vitric Andosol, Leptosol and Andosols that compose the area (Arnalds, 1999; Arnalds, 2015). As rainfall and snow events are not completely distinguished in the precipitation chronicle provided by the IMO, the effective rainfall we calculate does not represent the effect of the snow melt (delayed recharge to the aquifers).

The thicknesses of the geological formations were estimated combining the thicknesses extracted from the existing geological logs and literature.

We calculated hydraulic conductivities with two different methods: from grain size data for the till and glacio-fluvial deposits and from slug tests for both aquifers. For the grain size data method, we used d_{10} from samples collected in the Skálafellsjökull area. Their representativeness is local and up to 2 m depth. We carried out the calculation using the modified Hazen formula, developed empirically (in various soil types in Northern Scotland, MacDonald et al., 2012) and applied on a glacierised valley very similar to the study area (Dochartaigh et al., 2019, Virkisjökull valley, Iceland):

$$\log(K) = 0.79 * \log(d_{10}) + 2.1 - 0.38 * SSD$$

with K the hydraulic conductivity in m.d^{-1}; d_{10} the threshold grain size under which 10 % of the grains are represented in mm; SSD the Soil State Description value, ranked between 0 and 1, from very loose to very dense state, here SSD = 1 (Dochartaigh et al., 2019).

We interpreted the slug tests with the Bouwer and Rice solution (Bouwer and Rice, 1976) for the unconfined boreholes (only on the rising parts of the tests) and with the Hvorslev method (Hvorslev, 1951) for the confined boreholes. The results are representative for a few meters distance in radius from the borehole and for the whole depth of the saturated screen in the borehole (table 1).

We estimated specific yield (S_y) for both aquifers using grain size data (graph in Robson, 1993) and the Water Table Fluctuation (WTF) method on distinct rainfall-recharge event after manual correction of the Lisse effect (Crosbie et al., 2005; Healy and Cook, 2002):

$$S_y = R / \Delta h$$

with R the recharge in m, and Δh the increase in groundwater table in m. Only recharge events due exclusively to rainfall should be considered, thus we excluded days with snow precipitation and/or snow cover, as well as periods of potential significant glacial melt recharge.

The topographic map used for the plain and the top of the glaciers is IslandsDEMv1 (fig. 1), a seamless and bias-corrected mosaic from ArcticDEM (Porter et al., 2018) and lidar (Jóhannesson et al., 2013) from the National Land

Survey of Iceland (IslandsDEMv1, Landmælingar Íslands), with a 2×2 m resolution and a vertical accuracy better than 0.5 m. The basal topography of the 4 studied outlet glaciers is known using radio-echo sounding measurements interpolated at a resolution of 200×200 m (Björnsson and Pálsson, 2020).

We used several free and open software packages: the Geographic Information System QGIS (QGIS.org, 2022) to update and create maps, as well as perform mathematical operations on maps; LibreOffice for statistical treatments and graphics drawing (Foundation, T.D., 2020); and Python (Python.org, 2022) for data analysis and graphics drawing.

4 New data

We present here the new data sets allowing the characterisation of the dynamic of each aquifer.

~~We present here the new data set allowing the characterisation of the dynamic of each aquifer.~~

4.1 Groundwater level

The groundwater level in the till and glacio-fluvial deposits aquifer is often near or at the surface topography. South of Fláajökull especially groundwater levels are very close to the topography (fig. 7), which is not a surprise as many temporary swamps can be found in this area. The county that contains this area is actually called "mýrar", which means swamps. Groundwater level amplitudes of the temporal variations are decreasing with the distance to the glacier (from 1.70 m in FLA4 to 0.30 m in FLA1). Uncertainties are lower than 6 cm, except for FLA3 where they are of the order of 13 cm.

The groundwater level in the basalt aquifer varies from -42 m b.g.l. (below ground level; 19 m a.s.l) in HA13 (fig. 8, in a topography slope at the bottom of a basalt cliff) to over the surface topography in some plain areas (ASK100 in Kálfafellsdalur valley, recurring artesian well, fig. 3), and a recurring spring in the plain between Skálafellsjökull and the coastline. In the plains, the confined parts of the basalt aquifer (HA16, ASK103 and ASK104, fig. 8) show groundwater level variations with much smaller amplitudes (0.4 to 0.6 m) than in the unconfined parts (over 1 m, boreholes ASK102 and ASK105, fig. 8). In the topography slopes at the bottom of the basalt cliffs the amplitude of the variations is much bigger (nearly 2 m to 4 m, boreholes HA13 and HA12, fig. 8). Uncertainties are lower than 6 cm for ASK013, ASK104 and HA16, and of the order of 15 cm for ASK102, ASK105, HA12 and HA13.
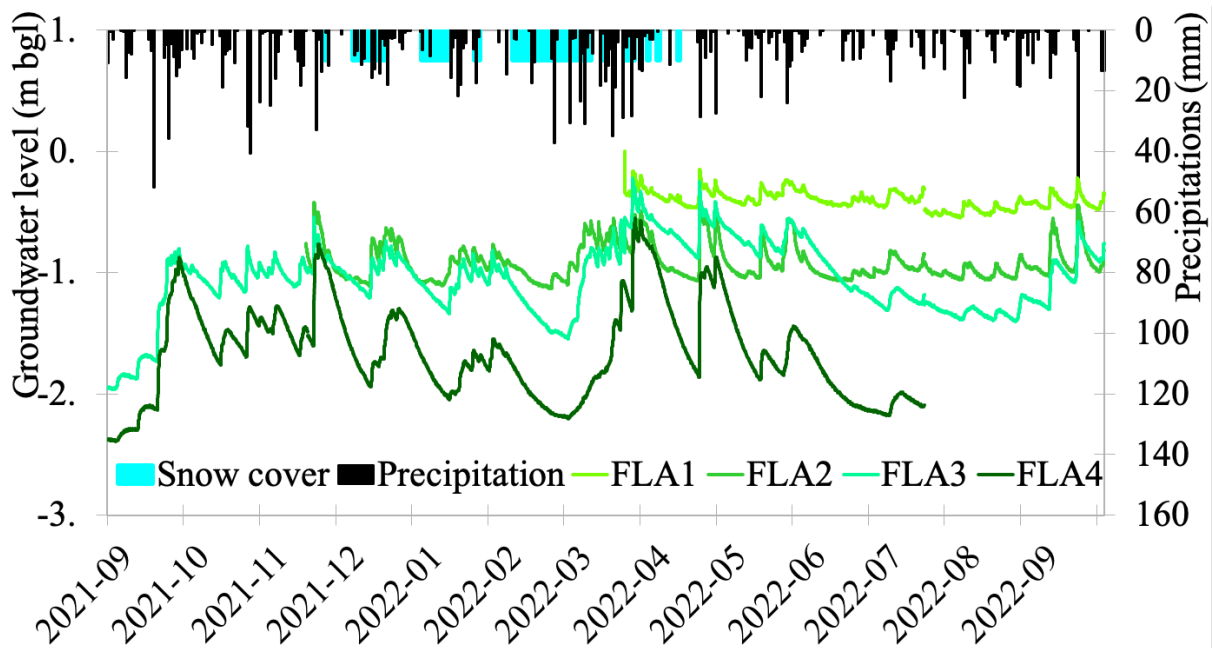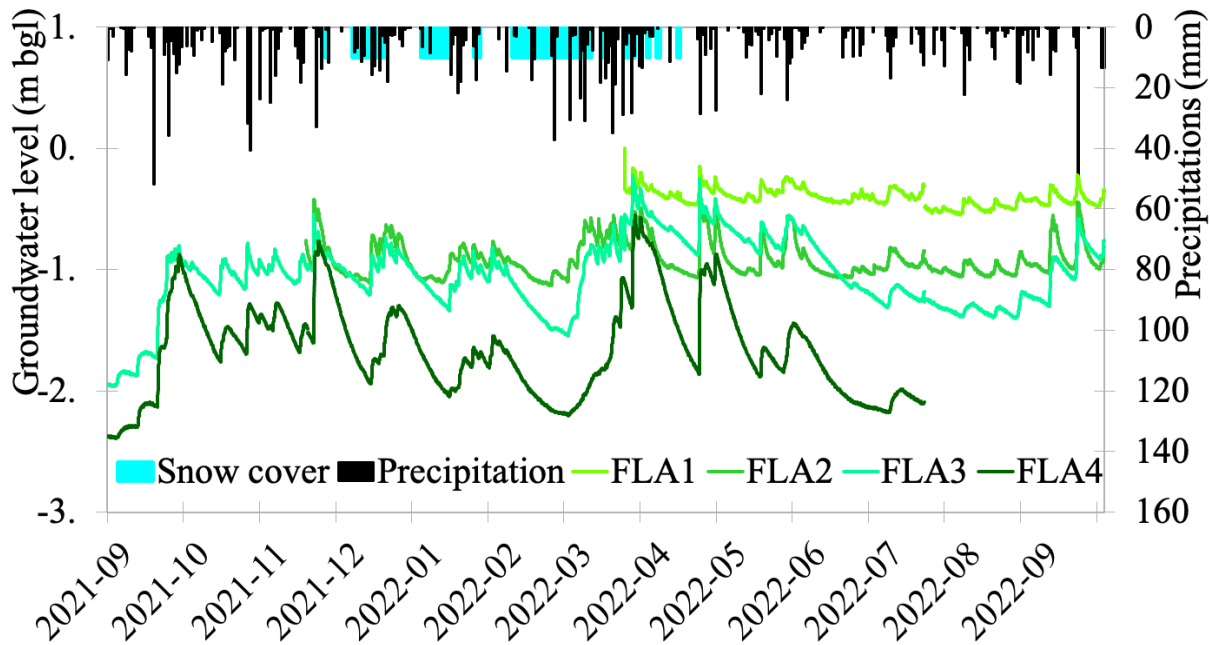
Figure 7: Hourly evolution of the groundwater level in the till and glacio-fluvial deposits aquifer south of Fláajökull, from August 2021 to September 2022 (in 4 boreholes: FLA1, FLA2, FLA3, FLA4, see fig. 3 for locations) in m b.g.l., and daily precipitation from Höfn weather station 705, and days with snow cover.

Fláajökull especially groundwater levels are very close to the topography (fig. 7), which is not a surprise as many temporary swamps can be found in this area. The county that contains this area is actually called "mýrar", which means swamps. Groundwater level amplitudes of the temporal variations are decreasing with the distance to the glacier (from 1.7 m in FLA4 to 0.3 m in FLA1).

13

Figure 8: Hourly evolution of the groundwater level in the basalt aquifer, from September 2021 to September 2022 (5 boreholes: ASK102, ASK103, ASK104, ASK105, HA16, see fig. 3 for locations) in m b.g.l., and daily precipitation from Höfn weather station 705, and days with snow cover.

4.2 Temperature

Hourly temperatures have been recorded in ten boreholes: FLA2, FLA3 and FLA4 in the till and glacio-fluvial deposits aquifer, and ASK102, ASK103, ASK104, ASK105, HA12, HA13 and HA16 in the basalt aquifer (location on fig. 3), with an uncertainty below 0.2 degrees Celsius. In the till and glacio-fluvial deposits aquifer the temperature tends to follow the trends of the atmospheric temperature with a lag of about six weeks: globally decrease from September to March and increase from April to September, covering a range of 1–9 °C (fig. 9). Several plateaux of temperature around 5 °C are visible on the record of FLA4, the closest borehole to Fláajökull glacier, and are interpreted in sect. 5.2.4. All the probes in boreholes in the basalt aquifer at less than 10 m b.g.l. (all boreholes except HA13) display a narrow range of values, 5–9 °C.
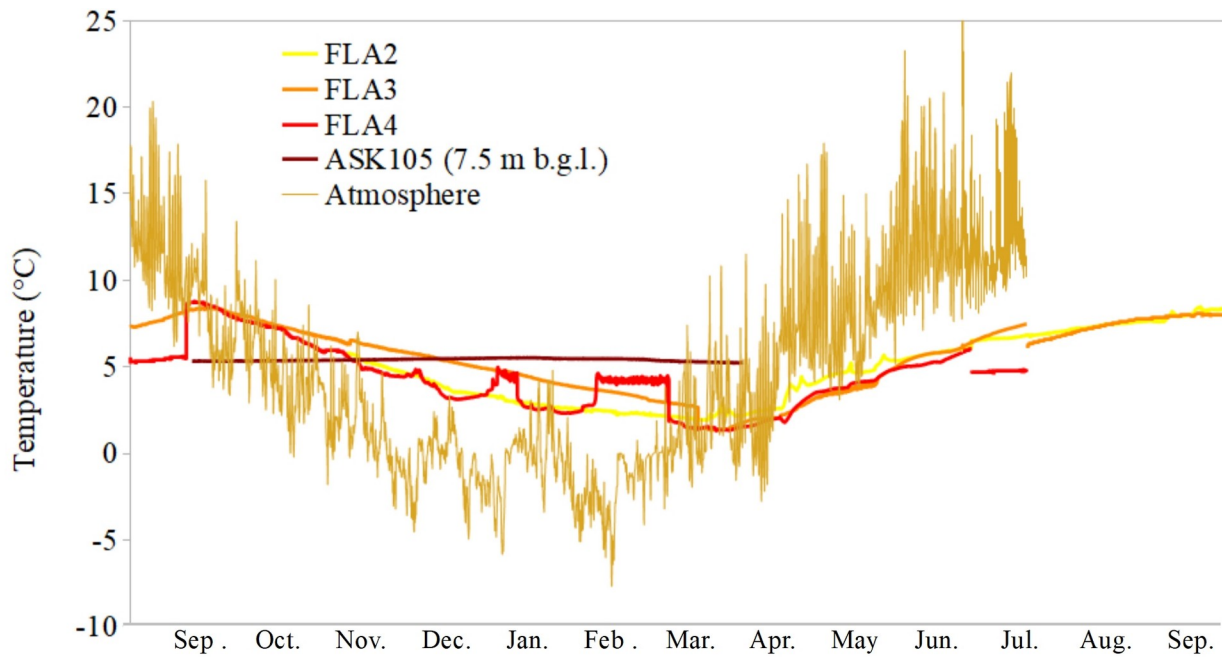
Figure 9: Hourly temperature from August 2021 to September 2022: in the till and glacio-fluvial deposits aquifer in 3 boreholes (FLA2, FLA3, FLA4), in the basalt aquifer in 1 borehole (ASK105 at 7.5 m b.g.l.), and in the atmosphere (recorded by a Baro Diver at the top of FLA4). See fig. 3 for locations of the boreholes.

4.3 Electro-conductivity

Water with an EC < 700 µS cm^{-1} is considered non-saline, between 700 and 2000 µS cm^{-1} slightly saline and between 2000 and 10 000 µS cm^{-1} moderately saline (Rhoades et al., 1992). Values of EC above 700 µS cm^{-1} have been measured in three boreholes, by order of decreasing values: VG1, HA16, and HA23 (table 2). Values measured in HA26 are just below or just over 700 µS cm^{-1}. In ASK104, groundwater is completely fresh until -8 m b.g.l., but below that level, EC values are significantly above 700 µS cm^{-1}. These boreholes are close to the coastline or to the brackish lake connected to the sea (fig. 3). The closer they are to one or the other, the higher their EC values are. EC has also been measured hourly in HA16 from May to September 2022: EC is varying from 700 to 1850 µS cm^{-1} with regular cycles (period of 24 hours due to the tide and period of 3 to 4 days).

15

360

EC (µS cm⁻¹)	**HA16**	**HA23**	**HA26**	**VG01**	**ASK104 (at 9 m depth)**
08/2021	2600	1300	900	4400	1400
09/2021	2200	1100	700	5600	_
03/2022	4700	_	_	6200	2600
05/2022	1800	_	500	2600	_
06/2022	_	_	600	3000	_
07/2022	_	_	600	2900	_
09/2022	1900	1200	600	3900	1800

Table 2: Electro-conductivity (EC) values (µS cm⁻¹) higher than 700 measured in boreholes in the study area from August 2021 to September 2022; _: no measurement available. For location see fig. 3. Uncertainties +/- 100 µS cm⁻¹.

365

4.4 Slug tests

Table 3 summarizes the results of the slug tests conducted in 11 boreholes. Hydraulic conductivities (K) of till and glacio-fluvial aquifer range from 5.8E-6 m s⁻¹ to 3E-5 m s⁻¹ while those of basalt aquifer range from 1.1E-10 to 4.9E-6 m s⁻¹. Thus, there is a wider heterogeneity of K in the basalt aquifer, which can be easily explained by its fractured nature.

370

Borehole	Formation	(Un)confined	Number of tests	Analysis method	K (m s⁻¹)	+/-	Distance to the glacier front (m)
ASK113	Till and g-f	unconfined	6	Bouwer and Rice	**5.8E-6**	1.5E-7	6420
FLA1	Till and g-f	unconfined	6	Bouwer and Rice	**5.8E-6**	1.5E-6	6350
FLA2	Till and g-f	unconfined	3	Bouwer and Rice	**6.9E-6**	1.0E-6	4520
FLA3	Till and g-f	unconfined	3	Bouwer and Rice	**1.7E-5**	4.9E-6	3280
FLA4	Till and g-f	unconfined	6	Bouwer and Rice	**3.0E-5**	1.1E-6	2740
ASK101	Basalt	confined	1	Hvorslev	**1.1E-10**	-	
ASK102	Basalt	unconfined	3	Bouwer and Rice	**8.5E-8**	3.8E-8	
ASK103	Basalt	confined	4	Hvorslev	**2.9E-7**	1.0E-7	
ASK105	Basalt	unconfined	5	Bouwer and Rice	**5.4E-8**	5.8E-8	
HA16	Basalt	confined	2	Hvorslev	**8.6E-7**	8.6E-7	
RV09	Basalt	confined	5	Hvorslev	**4.9E-6**	1.8E-6	

Table 3: Results of the slug tests conducted in July and September 2022. For each borehole in which tests were conducted, are listed the aquifer tapped, the confined or unconfined status of the tapped aquifer, the number of tests, the method of analysis

375

used to interpret the slug tests data, the average value of hydraulic conductivity calculated from the data, the incertitude on this value, and the distance to the glacier front for the till and g-f aquifer. g-f: glacio-fluvial deposits.

5 Results

We will first detail the amounts of available water for surface flow and groundwater flow obtained, providing an upper limit for the recharge rates, then go through the characteristics of both aquifers, and finally their dynamic. ~~We will first detail the recharge rates obtained, then go through the characteristics and dynamic of both aquifers, and finally propose a conceptual model of the system.~~

5.1 Recharge estimation

5.1.1 Subglacial water flows~~recharge~~

The available water for surface flow and groundwater recharge in the subglacial area (table 4) is on average 4000 mm year^{-1}. During the period 2010–2016, the average available water quantity on each glacier obtained from the combination of the HIRHAM 5-ICRA results or the summer mass balance with the effective rainfall are very similar for Fláajökull (0 % difference) and Skálafells- and Heinabergsjöklar (10 % higher with the HIRHAM 5-ICRA results), but significantly higher for Breiðamerkurjökull, by 22 % (table 4). The subglacial recharge is highly seasonally variable and peaks in July and August (fig. 10). An example of the available subglacial water according to the elevation is reported in table 5. As can be expected, because og higher melt rates at lower elevation, the available subglacial water is much higher under the lowest elevation of the glaciers for both sets of results. The subglacial recharge thus varies temporally and in space (elevation), and the available data and results allow to account for that.

Data set	Time period	Available subglacial water (mm year^{-1})		
		Breiðamerkurjökull (eastern part)	Skálafells &Heinabergsjöklar	Fláajökull
Summer Mass Balance	2010-2021	3600	4000	3800
	2010-2016	3600	4000	3800
	2021	3600	4200	4000
HIRHAM 5-ICRA results	2010-2016	4400	4400	3800

Table 4: Available water for subglacial flow over the ground and the groundwater flow in the subglacial area (mm year^{-1}), estimated: i) from summer mass balances (field data, IES Glaciology group) and effective rainfall, ii) from HIRHAM 5-ICRA results (Schmidt et al., 2020) and effective rainfall, for each outlet glacier considered.

~~The subglacial recharge rate (table 4) is in average 2000 mm year^{-1}. During the period 2010–2016, the average recharge rate on each glacier obtained from the combination of the PISM-ICRA results or the summer mass balance with the effective rainfall are very similar for Fláajökull (0 % difference) and Skálafells- and Heinabergsjöklar (10 % higher with the PISM-ICRA results), but significantly higher for Breiðamerkurjökull, by 22 % (table 4). The recharge under the glacier is highly seasonally variable and peaks in July and August (fig. 10). An example of the subglacial recharge according to the elevation is reported in table 5. As can be expected, the recharge is much higher under the lowest elevation of the glaciers for both sets of results. The subglacial recharge thus varies temporally and in space (elevation), and the available data and results allow to account for that.~~

17

Subglacial recharge (mm year^{-1})				
Data set	Time period	Breiðamerkurjökull (eastern part)	Skálafells &Heinabergsjöklar	Fláajökull
Summer Mass Balance	2010-2021	1800	2000	1900
	2010-2016	1800	2000	1900
	2021	1800	2100	2000
PISM-ICRA results	2010-2016	2200	2200	1900

Table 4: Recharge to the aquifers (mm year^{-1}), estimated: i) from summer mass balances (field data, IES Glaciology group) and effective rainfall, ii) from PISM-ICRA results (Schmidt et al., 2020) and effective rainfall, for each outlet glacier considered.
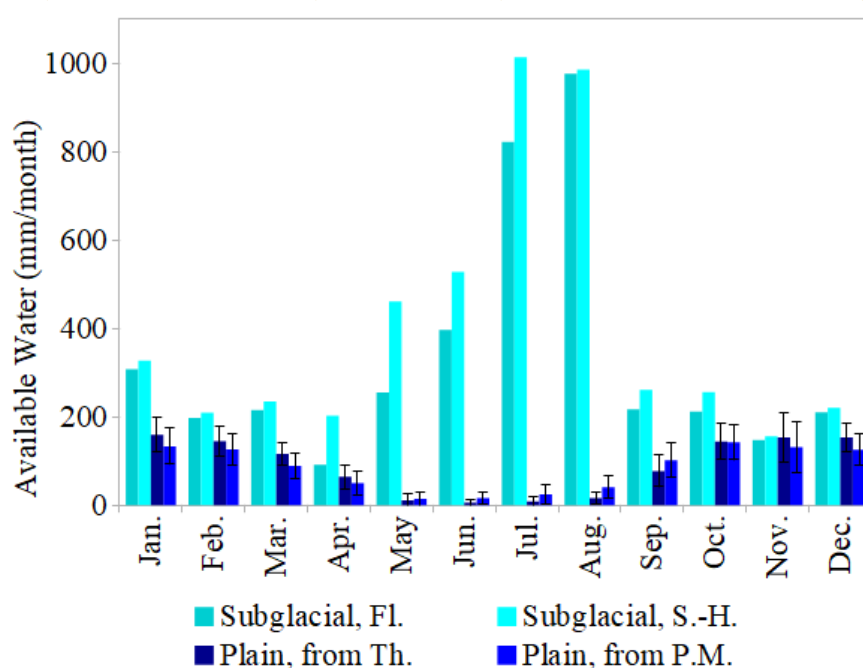
Figure 10: Monthly available waterrecharge in the plain and under the glaciers: (i) In the plainPlain recharge, average on 1990-2021, calculated from monthly precipitation (from combined Höfn weather stations) and monthly potential evapotranspiration calculated with Thornthwaite method (Th., monthly standard deviation between 3015 and 19296 mm) and with Penman-Monteith method (P.M., monthly standard deviation between 5428 and 228114 mm); (ii) Subglacial recharge, estimated from the melt SNMELT variable (run HIRHAM 5PISM-ICRA 2012 projected with the 2021 total summer mass balance) and the effective rainfall, under Fláajökull (Fl.) and Skálafells-Heinabergsjöklar (S.-H.).

Fláajökull Subglacial recharge, 2010 (mm year^{-1})		
Elevation (m a.s.l.)	From summer mass balance	From HIRHAM 5-ICRA results
1300 – max.	1800	2000
1100 – 1300	2800	2400
900 – 1100	3600	2600
700 – 900	4800	4000
500 – 700	5400	5400
0 – 500	7200	6400
Fláajökull Subglacial recharge, 2010 (mm year^{-1})		
Elevation (m a.s.l.)	From summer mass balance	From PISM-ICRA results
1300 – max.	900	1000
1100 – 1300	1400	1200
900 – 1100	1800	1300
700 – 900	2400	2000

| 500 – 700 | 2700 | 2700 |
| 0 – 500 | 3600 | 3200 |

Table 5: Available subglacial water Subglacial recharge rates to the aquifers (mm year⁻¹) according to the elevation, estimated from summer mass balances and HIRHAM 5PISM-ICRA results. Example of one year (2010) for one glacier (Fláajökull) to give an insight of the variations of the recharge rates with the elevation.

5.1.2 In the plain

The total effective rainfall, based on the PETotential Evapotranspiration calculated with Thornthwaite method, has increased by 165 mm (from 975 to 1140) since 1990, following the precipitation trend (fig. 4).

The monthly variation of the effective rainfall, based on the PETotential Evapotranspiration (PET) calculated from 1990 to 2021, shows that several months each year have no effective rainfall at all (PET with Thornthwaite method: 2–5 months, very rarely none; Penman-Monteith method: 1–4 months, very rarely 0, 5 or 7 months). Months with no effective rainfall are most of the time between April and August. These months have an inter-annual average of effective rainfall < 30 mm. The winter's months, October to March, all have an average effective rainfall above > 100 mm, with a maximum in January and February.

Water available in the area between the glaciers terminus and the coastline (mm year⁻¹)	From PET calculated with Thornthwaite method			From PET calculated with Penman-Monteith method		
	1990-2019	2020	2021	1990-2019	2020	2021
	1020	1120	900	970	900	830
Uncertainties	+/- 280			+/- 360		

Table 6: Effective rainfall, or Water available (mm year⁻¹) in the plain (between the glaciers terminus and the coastline) for both surface runoff and recharge to the aquifers.

The estimation of the recharge of the aquifers occurring between the glacier terminus and the coastline (i.e. the plain) is based on the effective rainfall. The surface runoff being important, and with a lack of data allowing a more accurate estimation, a scaling coefficient of 0.5 (with a range of 0.25–0.75) is applied to the effective rainfall to obtain the recharge rate (table 6).

Scaling coefficient applied to the effective rainfall	Recharge in the area between the glaciers terminus and the coastline (mm year⁻¹)					
	From PET calc. with Thornthwaite method			From PET calc. with Penman-Monteith method		
	1990-2019	2020	2021	1990-2019	2020	2021
25%	260	280	220	360	220	210
50%	510	560	450	480	450	410
75%	760	840	670	730	670	620

Table 6: Recharge to the aquifers (mm year⁻¹) in the plain (between the glaciers terminus and the coastline), estimated from the effective rainfall. The ratio applied to the effective rainfall to obtain the recharge rate is 50%, and is made to vary to 25 % and 75 % for sensibility tests. calc.: calculated.

On the plain the interannual average hydrologic balance on 1990–2021 is the following: 1540 mm (± 310 mm) of precipitations, 520 mm (± 80 mm) of evapotranspiration (both methods used), 1000500 mm (± 300150 mm) of water available for runoff and forand 500 mm (± 150 mm) of recharge to the aquifers.

19

5.2 Aquifers characteristics

5.2.1 Geological formations thicknesses

Subglacial till formation is from 1 to 20 m thick (average 5 m) under Skálafellsjökull (estimates based on Ground Penetrating Radar, Hart et al., 2015; Hart, 2017). Immediate proglacial till, which can be a good representation for subglacial ones, have a thickness up to 3 m in front of Skálafellsjökull (Hart, 2017), between 3.5 and 5 m in front of Fláajökull (Evans and Hiemstra, 2005). The thickness probably varies and the subglacial till might even not be continuous everywhere.

In the plain the till and glacio-fluvial deposits formation total thickness is from 2 to 54 m (maximum in RV08) with an average of 15 m, according to the drilling logs of 16 boreholes consulted (locations on fig. 6). This interval is confirmed by 5 m of till and glacio-fluvial deposits in a borehole in Hali (HA25, Sigurðarson et al., 2016) and a 16 m high stratigraphic log full of sediments in a cross section along the Kolgríma river, close to the Skálafellsjökull terminus (Evans et al., 2000). Thicknesses are much more important south of Breiðamerkurjökull, with a thickness of till and glacio-fluvial deposits between 30 m and 150 m, from the glacier to the coastline (seismic reflection and refraction measurements, Bogadóttir et al., 1987; Boulton et al., 1982).

A basalt formation has generally a high contrast in hydraulic conductivity (K) from top to bottom, as with time and a temperature over 50 °C the fractures are filled with secondary minerals, products of the chemical alteration (smectite, illite, zeolite at low temperatures and chlorite and epidote for higher grade metamorphism, e.g. Arnórsson, 1995). Thus we consider that lower than the 50 °C isotherm the hydraulic conductivity of the basalt formation becomes negligible. The depth of the 50 °C isotherm can be estimated using the drilling logs consulted at RFS and to data presented in Sigurðarson et al., (2016), who provide detailed analysis of geophysical measurements in the borehole HA25 in Hali. The temperature log of borehole HA25 indicates 51 °C at -303 m, but both the stratigraphic description and the deviations in geophysical measurements show a shallower boundary at -194 m (Sigurðarson et al., 2016). From the drilling logs consulted at RFS, we have identified temperatures over 50 °C only in HA14: 53 °C at -384 m (43 °C at -186 m), suggesting a boundary at nearly -400 m. No temperature over 50 °C are observed in HA18 (on 180 m,), RV08 (on 340 m), RV11 (on 143 m), suggesting the 50 °C isotherm is not above at least -140 m. Furthermore, weathered materials are described in VG03 (precipitate from 173 m to 200 m), suggesting a transition at 200 m, and in RV10 (dark shale at 709 m). Thus the present 50 °C isotherm is between -300 and -400 m, and the boundary with older altered areas brought nearer to the surface by glacial erosion is around -200 m. The bottom of the basalt aquifer can thus be considered to be between -200 m and -400 m below the surface or the bottom of the till and glacio-fluvial deposits.

5.2.2 Aquifers hydraulic conductivity

The hydraulic conductivity (K) values of the till and glacio-fluvial deposits calculated from grain size data (fig. 11) vary from 4.5E-6 to 3E-5 m s^{-1}, (for respectively average d_{10} of 2 and 22 μm). This is in the range of values found in the literature for Iceland: from 1E-6 m s^{-1} (Iverson et al., 2017, Múlajökull till) to 7E-4 m s^{-1} (Dochartaigh et al., 2012, Virkisjökull, glacial till, max. measured). The value of 3E-5 m s^{-1} is very close to the 3.8E-5 m s^{-1} calibrated for the Virkisjökull sandur (Mackay et al., 2020). Measurements done via slug tests yield similar results as the ones calculated from grain size data: 1.5E-5 [5.8E-6–3E-5] m s^{-1}. They moreover show a decreasing trend from the glacier toward the

coastline (table 3), which can results from the decrease of grain size from the glacier terminus to the coast, due to fluvial transport.
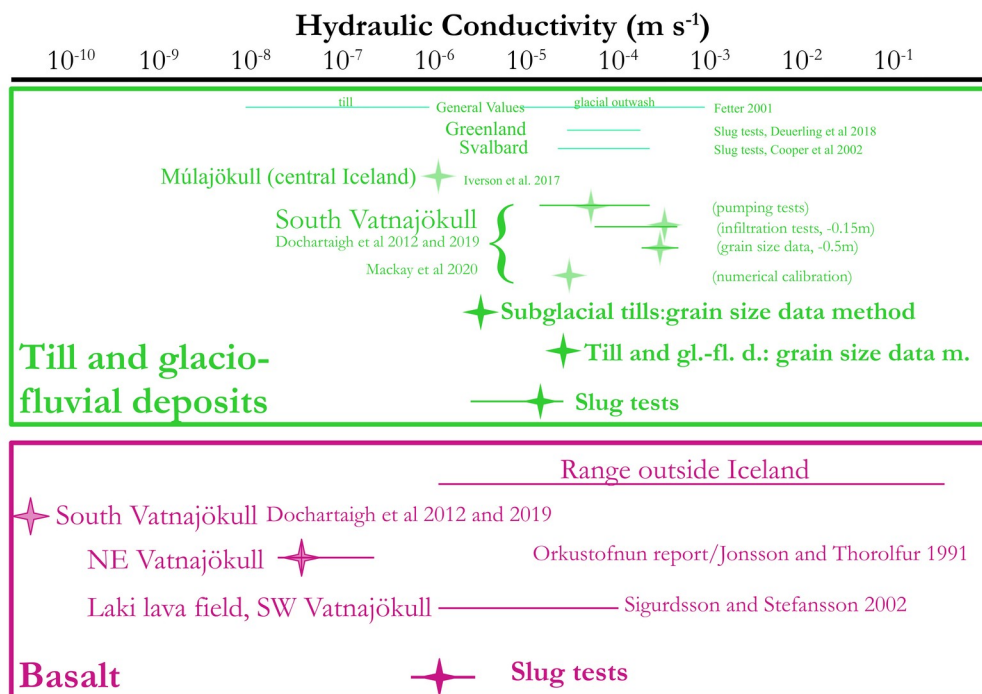
~~The hydraulic conductivity (*K*) values of the till and glacio-fluvial deposits calculated from grain size data (fig. 11) vary~~
~~from 4.5E-6 to 3E-5 m s⁻¹, (for respectively average d_{10} of 2 and 22 µm). This is in the range of values found in the~~
~~literature for Iceland: from 1E-6 m s⁻¹ (Iverson et al., 2017, Múlajökull till) to 7E-4 m s⁻¹ (Dochartaigh et al., 2012,~~
~~Virkisjökull, glacial till, max. measured). The value of 3E-5 m s⁻¹ is very close to the 3.8E-5 m s⁻¹ calibrated for the~~
~~Virkisjökull sandur (Mackay et al., 2020). Measurements done via slug tests yield similar results as the ones calculated~~
~~from grain size data: 1.5E-5 [5.8E-6–3E-5]. They moreover show a decreasing trend from the glacier toward the~~
~~coastline (table 3), which can results from the decrease of grain size from the glacier terminus to the coast, due to fluvial~~
~~transport.~~

Hydraulic conductivities (*K*) values for the basalt formation calculated with the data from the slug tests are presented in table 7 and fig. 11. They fall in the range of bibliographical values for basalt *K* in Iceland (fig. 11). Outside Iceland, *K* values for basalt can be found from 1E-6 to 6E-1 m s⁻¹ (fig. 11) and show the heterogeneous character of this type of formation. Higher values are found in fissured and young basalts, while lower ones are found in the core of lava flows, weathered and old lavas. This range is based on the following references: Columbia River Plateau (USA), on a 1 to 5 km thick Miocene plateau, with 800 bulk *K* measurements in 577 wells on the first 500m: 6E−5 to 6E−1 m s⁻¹, vertical *K* 5 times smaller (Jayne and Pollyea, 2018); La Réunion, 6E-4 to 3E-1 m s⁻¹ (Join, 1991), 1E-3 m s⁻¹ (numerical model calibration) (Violette et al., 1997); Mayotte, in situ measures in lava flow: massive <1E-6, scoriated: 5E-6 to 5E-4, fissured: 1E-6 to 5E-4 m s⁻¹ (Lachassagne et al., 2014). In Iceland *K* values for basalt vary on 7 orders of magnitude (fig. 11): less than 1E-10 m s⁻¹ (Dochartaigh et al., 2012 and 2019: Virkisjökull glacier in south-eastern Iceland, through constant rate pumping tests of 3 to 6 hours), 2E-8 to 5E-8 m s⁻¹ (Jonsson and Thorolfur, 1991: boundary between the mountainous East Fjords and the high plateau of central Iceland), 5E-10 to 1E-4 m s⁻¹ (Aggarwal, 2020: Laki lava field).

Figure 11: Hydraulic conductivity values for the till and glacio-fluvial deposits and the basalt from data analysis and the literature; stars indicate single or average value and horizontal lines the range of values measured. The range for hydraulic conductivities of basalt outside Iceland is based on several bibliographical references, details and references in the text.

5.2.3 Aquifers storage coefficients

Aquifer storage coefficient S is composed of two parts, specific yield S_y and specific storage S_s:
$S_y + S_s*e$ (e being the thickness of the aquifer), S_y being dominant in unconfined aquifers, and S_s*e dominant in confined aquifers. We calculated S_y using the WTF method for three to seven distinct rainfall-recharge events depending on the borehole and the length of the available groundwater record (table 7). Adequate data was available from four boreholes in the till and glacio-fluvial deposits (FLA1, FLA2, FLA3, and FLA4), and two in the basalt aquifer (HA13 and ASK102). Direct use of the WTF method from different values of S_y show that values greater or equal to 0.12 for the till and glacio-fluvial deposits and 0.11 for the basalt imply a recharge larger than the measured precipitation, thus setting an upper limit to the possible interval for S_y. The conclusion is that till and glacio-fluvial deposits $S_y \in$ [0.01–0.12] and basalt $S_y \in$ [0.02–0.11].

	from Grain size data		From WTF method	From the literature
Geological formation	interval d_{90} (µm)	S_y (-)	S_y (-)	S_y (-)
Proglacial till and gl.-fl. d.	120–760	0.12–0.32	0.05 (+/- 0.05)	0.06–0.16 (Morris and Johnson, 1967)
Basalt	_	_	0.03 (+/- 0.01)	0.08 (Heath, 1983)

Table 7: Specific yield (S_y) values calculated using: (i) for the till and glacio-fluvial deposits only, an estimate from grain size data; (ii) for both the till and glacio-fluvial deposits and the basalt, the Water Table Fluctuation (WTF) method on up to 7 rainfall-recharge events in October 2021 and April and May 2022, average (+/- standard deviation); gl.-fl. d.: glacio-fluvial deposits.

5.3 2.4 Aquifers dynamics

In the studied area groundwater is flowing towards the sea. Hydraulic gradients can be deduced from the difference of groundwater levels between two boreholes on the same potential groundwater flow line. Hydraulic gradient in the till and glacio-fluvial deposits aquifer is around 4.5/1000 south of Fláajökull. Hydraulic gradient in the basalt aquifer is around 3.5/1000 south of Fláajökull, around 3.9/1000 south of Skálafellsjökull and around 30/1000 in Hali.

Time evolution of the groundwater level in the till and glacio-fluvial deposits aquifer show clear recharge events by rainfall, by snow melt, and by glacial meltwater. Recharge by rainfall events occur within 24 hours of the precipitation event, at least when the rain is > 10 mm (fig. 7 and 8). Snow melt events are identified in February-March 2022 (fig. 7 and 8), and also on a shorter time scale in January 2022. When precipitation is snowfall and the snow cover last for more than one day, the lag between a snowfall precipitation event and the recharge of the groundwater is visible (fig. 7 and 8), corresponding to the time for the snow to melt. In September the quicker increase of the water level in borehole FLA3 (+ 0.54 m from 30 August 2022 to 21 September 2022) compare to FLA2 and FLA1 (respectively + 0.21 m and + 0.11 m during the same period; fig. 7) demonstrates recharge by glacial meltwater. Similarly in the basalt aquifer (fig. 8) the trend line of the water level in borehole ASK105 show an increase of + 0.40 m from 17 August 2022 to 19 September 2022 that can not be accounted for only by the precipitation events during the same period. ASK105 lies at 4.2 km from the nearest glacier terminus; boreholes further away show a similar but smaller increase during the same period of time: ASK103 at 6.2 km: +0.2 m; ASK102 at 7.4 km: +0.22 m; HA16 at 7.4 km: +0.19 m.

Temperature data from FLA4 borehole exhibit 4 plateaux (constant value over a period of time) of temperatures between 4.2 to 5.4 °C (fig. 12). These plateaux correspond to every time the water level is lower than 24.1 m a.s.l. (fig. 12). We interpret that as an upward leakage from the basalt aquifer, triggered when the water level in the till and glacio-fluvial deposits aquifer is lower than the piezometric level in the confined basalt aquifer. The groundwater level in the basalt aquifer must then be very constant. The temperature measured in the basalt aquifer in ASK105 (1.6 km from FLA4), from 5 to 9 °C, corroborates that hypothesis.

The clear separation of both aquifers, and the confined character of the basalt aquifer observed in some locations, lead us to hypothesize the presence of a much less permeable layer between the till and glacio-fluvial deposits and the basalt formation. It could be a clay layer or a more compacted level of till.

At the coastline, 3 hypothesis can be made for the fresh/marine groundwater interfacing in each aquifer: equilibrium around the coastline, fresh groundwater pushing the interface offshore or marine intrusion inland. The few data acquired on the EC of the groundwater (high EC values near the coastline, table 2) suggest a potential seawater intrusion in the basalt aquifer. For the he till and glacio-fluvial aquifer we expect that some fresh groundwater is flowing into the sea.
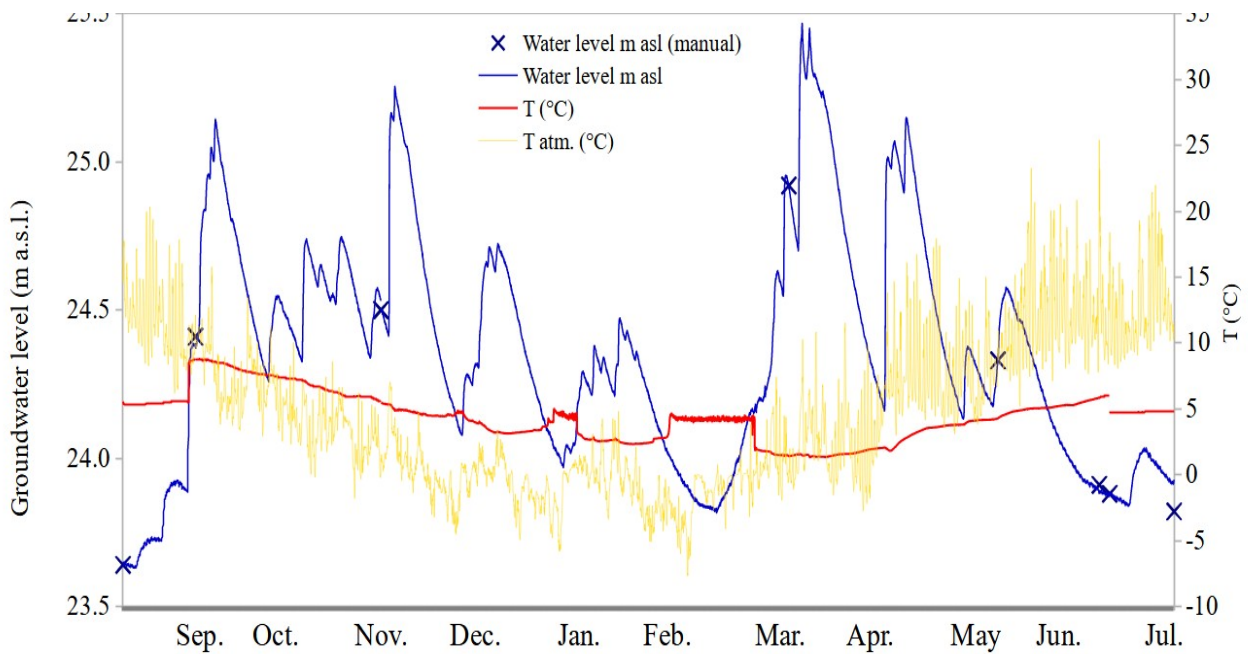
The high EC values near the coastline (table 2) suggest a potential seawater intrusion.

Figure 12: Hourly groundwater level (in blue, m a.s.l.) and temperature (in red) in the borehole FLA4, and atmospheric temperature (in yellow, from the Baro Diver probe in borehole FLA4). The temperature chronicle exhibits plateaux around 5 °C at the end of August 2021, in January, February and July 2022, each time the groundwater level is lower than 24.1 m a.s.l.

6. Discussion and5.3 Conceptual model

The recharge rates to the aquifers are estimated using the following assumptions. Between the glacier terminus and the coastline (i.e. in the plain), a scaling coefficient varying of 0.5 (with a range of 0.25–0.75) is applied to the effective rainfall. This coefficient is based on field observations (important surface runoff), and in the absence of surface flow record allowing a more accurate estimation (table 8). The interannual average hydrologic balance averaged

on 1990–2021 on the plain can thus be detailed as the following: 1540 mm (± 310 mm) of precipitations, 520 mm (± 80 mm) of evapotranspiration (both methods used), 500 mm (± 150 mm) of runoff and 500 mm (± 150 mm) of recharge to the aquifers. In the subglacial area, we can consider that half of the melt obtained infiltrates to the aquifers, with an uncertainty of 50%. This ratio is deduced from a 2012-2013 surface runoff data set (Young et al., 2015). In this study a 67.3 km^2 catchment of the glacier is studied, with daily surface runoff measurements in a river south of Skálafellsjökull, discharge which is assumed equal to the discharge emerging 500 m upstream from under the glacier (Young et al., 2015). The surface runoff measured and extrapolated (for days without data) accounts for 50 % (± 10%) of the volume of ice melt during the same period.

Scaling coefficient applied	Recharge in the area between the glaciers terminus and the coastline (mm year^{-1})					
	From PET calc. with Thornthwaite method			From PET calc. with Penman-Monteith method		
	1990-2019	2020	2021	1990-2019	2020	2021
25%	260	280	220	360	220	210
50%	**510**	**560**	**450**	**480**	**450**	**410**
75%	760	840	670	730	670	620

	Subglacial recharge (mm year^{-1})			
	From Summer Mass Balance			From HIRHAM 5-ICRA results
	2010-2021	2010-2016	2021	2010-2016
25%	1000	1000	1000	1100
50%	**1900**	**1900**	**2000**	**2100**
75%	2900	2900	3100	3200

Table 8: Recharge to the aquifers (mm year^{-1}) in the plain (between the glaciers terminus and the coastline), estimated from the effective rainfall, and in the subglacial area, estimated from: i) from summer mass balances (field data, IES Glaciology group) and effective rainfall, ii) from HIRHAM 5-ICRA results (Schmidt et al., 2020) and effective rainfall. calc.: calculated.

The subglacial recharge rate is on average 2000 mm year^{-1} and in the plain 500 mm year^{-1} (table 8). Thus recharge under the glacier is 4 times higher than the one on the plain, which is consistent with studies claiming a high recharge of the till and glacio-fluvial deposits aquifer by the melting of the glaciers (Sigurðsson, 1990; Xiang et al., 2016), while offering additional quantitative comparison. Following the patterns of the available water for both subglacial runoff and groundwater recharge (see fig. 10 and table 5), the recharge under the glacier is highly seasonally variable (4 times more in July-August than the rest of the year), and is much higher under the lowest part of the glaciers.

Figure 13 presents the conceptual model of the groundwater dynamic in glacierised basins deduced from all the data presented in this paper. A glacier with crevasses and moulins is represented, along with the two geological formations underlying it and in its front: the till and glacio-fluvial deposits and the basalt formation. The average characteristics of the geological formations are described along with their variability range. The subglacial recharge and recharge on the plain are quantified and their monthly variability specified. The groundwater dynamic is expressed by arrows. The water is entering the basin as precipitations, immediately joining the hydrologic and hydrogeological system if rainfall, or joining it delayed through melted snow and melted ice. The general flow direction of both the surface water and the groundwater is from the highest elevations (top of the glacier or top of the underlying bedrock) towards the coastline. Exchanges (between the subglacial hydrology network and the till and glacio-fluvial aquifer occur, as well as between the surface hydrology network and the till and glacio-fluvial aquifer. Downward (recharge) and also upward exchanges occur between the tills and glacio-fluvial aquifer and the basalt aquifer.

		Till and gl-fl.d.	Basalt
e	m	2 – 54	200 – 400
K	m.s^{-1}	4.5E-6 – 3.7E-5	1E-10 – 4.9E-6
S$_y$	–	0,01 – 0,12	0,02 – 0,11
T	°C	1 – 9	5 – 9 (above 10 m b.g.l.)
EC	µS.cm^{-1}	60 – 450	60 – 6200

Plain recharge: ~500 mm year^{-1}

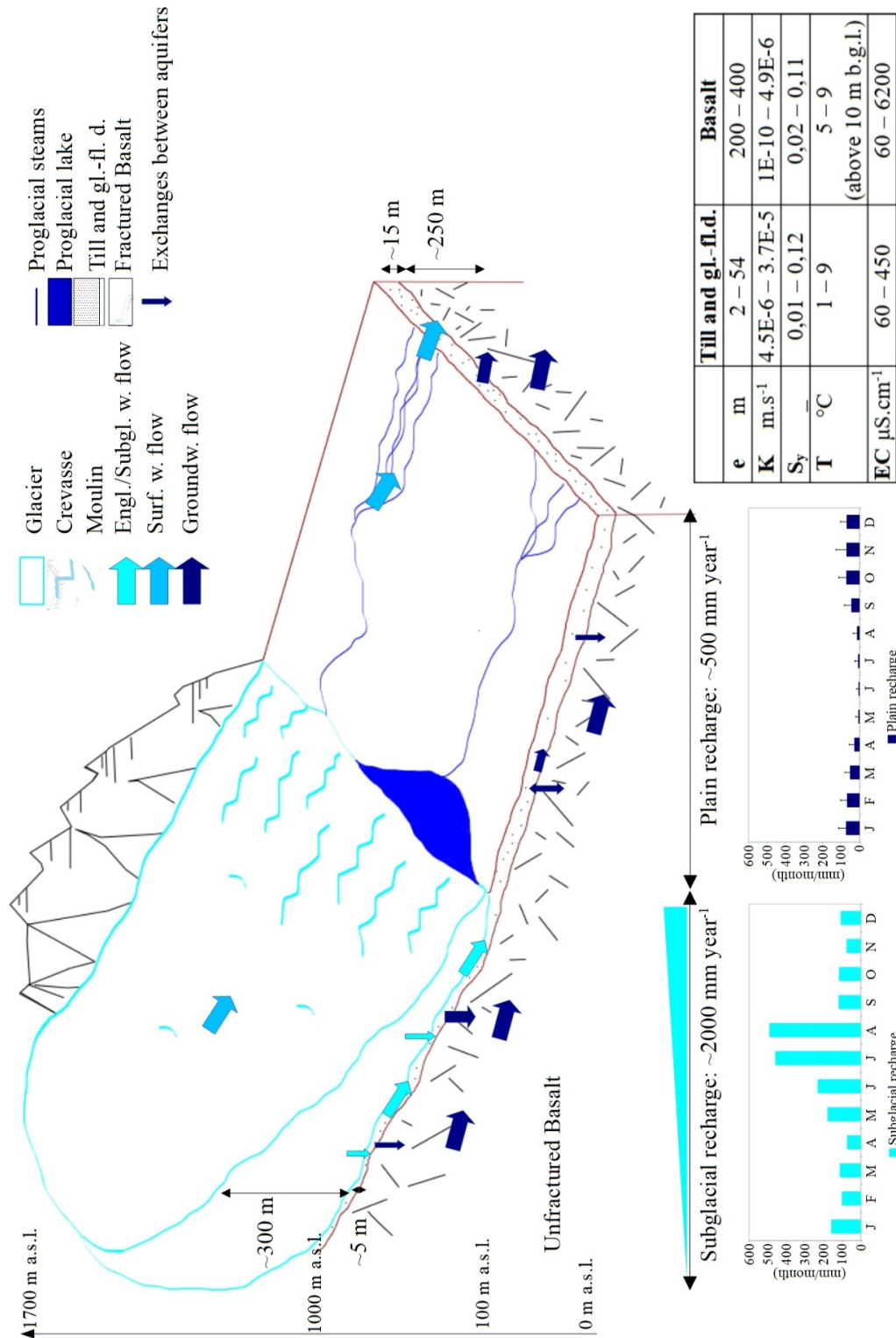Subglacial recharge: ~2000 mm year^{-1}

Figure 13: Conceptual model of the groundwater dynamic in glacierised basins such as those observed at Fláajökull, Heinabergsjökull and Skálafellsjökull. The model is based on all the data presented in this paper. A glacier is represented along with the two geological formations underlying it and in its front: the till and glacio-fluvial deposits and the basalt formation. Average characteristics of the geological formations are described along with their variability range, as well as recharge rates (subglacial and on the plain) along with their monthly variability. The groundwater dynamic is expressed by arrows. Subgl.: subglacial; w.: water; surf.: surface; groundw.: groundwater; gl.fl. d.: glacio-fluvial deposits.

595

600 Figure 13 presents the conceptual model of the groundwater dynamic in glacierised basins deduces from all the data presented previously. A glacier with crevasses and moulins is represented, along with the two geological formations underlying it and in its front: the till and glacio-fluvial deposits and the basalt formation. The average characteristics of the geological formations are described along with their variability interval. The subglacial recharge and recharge on the plain are quantified and their monthly variability specified. The groundwater dynamic is expressed by arrows.

		Till and gl.-fl.d.	Basalt
e	m	2 – 54	200 – 400
K	$m.s^{-1}$	4.5E-6 – 3.7E-5	1E-10 – 4.9E-6
S_y	–	0,01 – 0,12	0,02 – 0,11
T	°C	1 – 9	5 – 9 (above 10 m b.g.l.)
EC	$\mu S.cm^{-1}$	60 – 450	60 – 6200

~15 m ~250 m ~300 m ~5 m

Plain recharge: ~500 mm year⁻¹

Subglacial recharge: ~2000 mm year⁻¹

Unfractured Basalt

Plain recharge — (mm/month) — J F M A M J J A S O N D

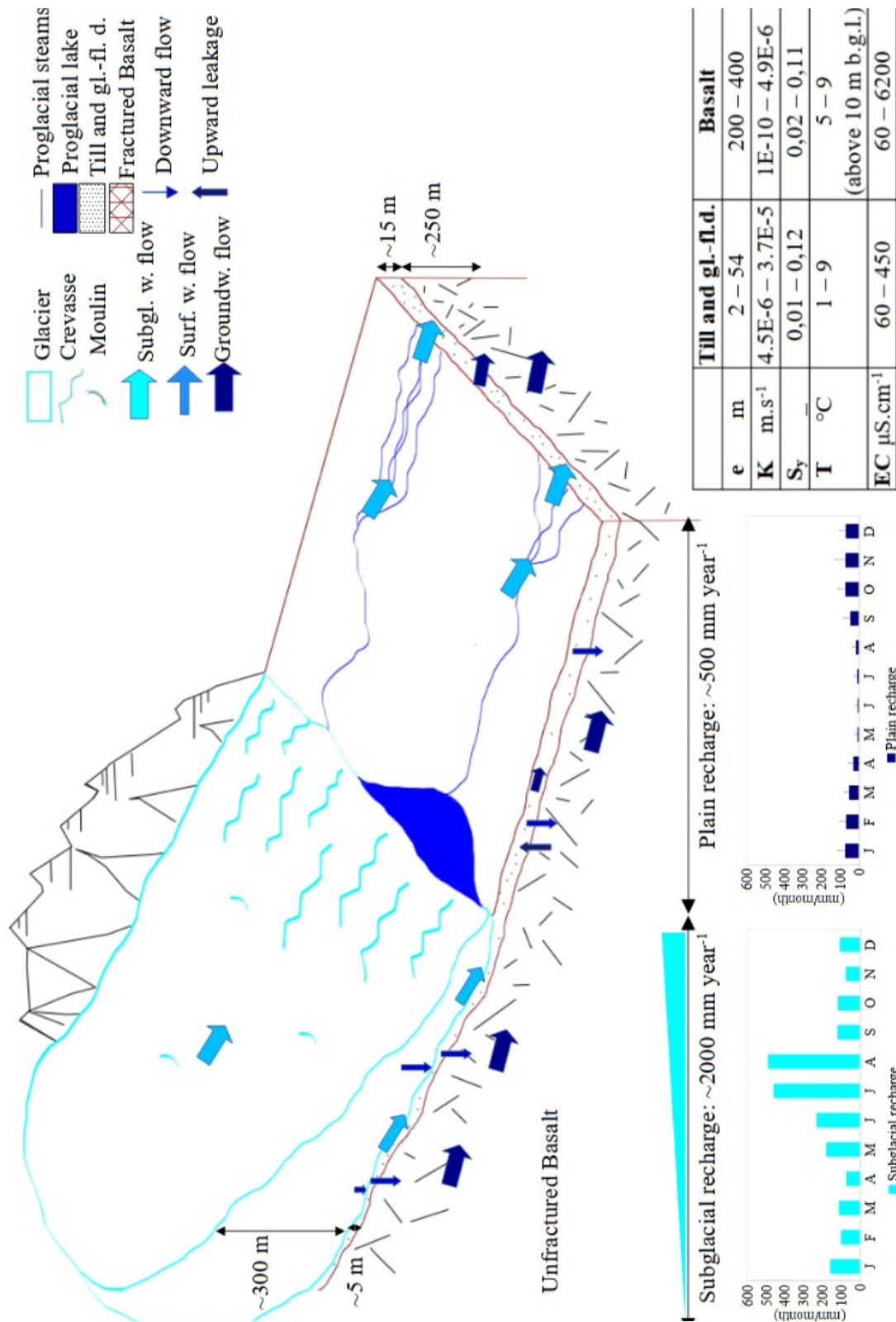Subglacial recharge — (mm/month) — J F M A M J J A S O N D

Figure 13: Conceptual model of the groundwater dynamic in glacierised basins such as those observed at Fláajökull, Heinabergsjökull and Skálafellsjökull. The model is based on all the data presented in this paper. A glacier is represented along with the two geological formations underlying it and in its front: the till and glacio-fluvial deposits and the basalt formation. Average characteristics of the geological formations are described along with their variability interval, as well as recharge rates (subglacial and on the plain) along with their monthly variability. The groundwater dynamic is expressed by arrows. Subgl.: subglacial; w.: water; surf.: surface; groundw.: groundwater; gl.fl. d.: glacio-fluvial deposits.

76 Conclusion

We have identified two di~~ffere~~stinct aquifers, one in the till and glacio-fluvial deposits and one in the basalts, with different hydrodynamic behaviour, using the geological map, and t~~hen~~he measurements in the boreholes of the established ~~new~~ observation network ~~established~~. For the till and glacio-fluvial deposits aquifer, we estimated a hydraulic gradient of 4 to 5/1000, and from 3 to 30/1000 for the basalt aquifer. By the borehole FLA4, when the water level in the till and glacio-fluvial deposits aquifer is lower than the piezometric level in the basalt aquifer, an upward leakage from the basalt aquifer takes place.

We have calculated the hydraulic conductivities and specific yields of both aquifers from field measurements: i) till and glacio-fluvial deposits: $K \in$ [4.5E-6–3.7E-5] m s^{-1}, $S_y \in$ [0.01–0.12]; ii) basalt aquifer: $K \in$ [1E-10–4.9E-6] m s^{-1}, $S_y \in$ [0.02–0.11]. These compare well with the values extracted from the scientific literature (fig. 11 and table 7). For the K of the basalt aquifer it is a much narrower range than in the literature, however the values we have gathered may not be enough to represent ~~its~~the geographical variability.

We have obtained a comprehensive water balance at the scale of the watershed, from the estimation of the water available for surface runoff and recharge of the aquifer system both under the glacier and on the plain. Subglacial recharge is estimated to be 4 times higher than the one on the plain, which is consistent with studies claiming a high recharge of the till and glacio-fluvial deposits aquifer by the melting of the glaciers. The subglacial recharge varies temporally (for 2021 maximum in July and August about 480 mm month^{-1}, and minimum in April and November, about 80 mm month^{-1}) and with the elevation (highest at the lowest glacier elevation 3400 mm year^{-1} in 2010, lowest at the highest elevation: less than 1000 mm year^{-1} in 2010).

~~We have obtained a comprehensive water balance at the scale of the watershed, from the estimation of the recharge of the aquifer system both under the glacier and on the plain. Recharge under the glacier is 4 times higher than the one on the plain, which is consistent with studies claiming a high recharge of the till and glacio-fluvial deposits aquifer by the melting of the glaciers (Sigurðsson, 1990; Xiang et al., 2016). The subglacial recharge varies temporally (for 2021 maximum in July and August about 480 mm month^{-1}, and minimum in April and November, about 80 mm month^{-1}) and with the elevation (highest at the lowest glacier elevation 3400 mm year^{-1} in 2010, lowest at the highest elevation: less than 1000 mm year^{-1} in 2010).~~

Several unknowns remain. The saturation of the till and glacio-fluvial deposits and basalt formations under the glacier is still to be directly measured~~remains unknown~~. The hypothesis of the presence of a clay layer or compacted till between the subglacial till and the basalt, and also between the till and glacio-fluvial deposits and the basalt formation, is to be confirmed. It would explain the separation of the two aquifers, and the confined character of the basalt aquifer observed in some locations. For the dynamic at the boundary with the sea we expect that some fresh groundwater from the till and glacio-fluvial deposits is flowing into the sea. A~~, for which a~~ hydrogeological model is required to calculate an estimate of the flux to the sea, and would also help test the hypothesis of a slight seawater intrusion in the basalt aquifer.~~.~~

We are thus developing numerical hydrogeological models that will allow further assessments of the remaining unknowns. Manual and automatic groundwater level measurements are to be continued for several years. Eventually, to further explore the potential feedback of the groundwater system on the glacier dynamics, a coupling of a glaciological model and the hydrogeological model would be necessary.

As demonstrated, subglacial recharge to aquifers is significant in contexts of~~involving~~ warm-based glaciers lying on sediments and/or fractured bedrock. It is thus important to include the groundwater component to~~artment to~~ evaluate accurately the water balance of glacierised catchments.

References

Aðalgeirsdóttir, G., Magnússon, E., Pálsson, F., Thorsteinsson, T., Belart, J. M. ~~M~~-C., Jóhannesson, T., Hannesdóttir, H., Sigurðsson, O., Gunnarsson, A., Einarsson, B., Berthier, E., Schmidt, L. S., Haraldsson, H. H., and Björnsson, H.: ~~,~~ ~~2020.~~ Glacier Changes in Iceland From ~1890 to 2019~~.~~, Front. Earth Sci., 8, 523646~~.~~, https://doi.org/10.3389/feart.2020.523646, 2020.

Aggarwal, A.: ~~, 2020.~~ Bypassing Barriers: Surface-Groundwater Exchange between a Wetland, Sandur, and Lava Field in South-Eastern Iceland, M~~M~~aster of Science, York University, 100 pp., 2020.

Anon: Python, 2022.

Anon: OR12088.pdf.

Anon: p.26 Summary of Surface measurement of permeability with Guelph permeameter: TO SEE IN DETAILS ??

Arnalds, Ó.: , 1999. Soil Survey and Databases in Iceland., Eur. Soil Bur. Res. Rep, 91–96, 1999.

Arnalds, O.: , 2015. The Soils of Iceland, SWorld Soils Book Series. Springer Netherlands, Dordrecht, 193 pp., https://doi.org/10.1007/978-94-017-9621-7, 2015.

Arnórsson, S.: , 1995. Geothermal systems in Iceland: Structure and conceptual models—I. High-temperature areas., Geothermics, 24, 561–602., https://doi.org/10.1016/0375-6505(95)00025-9, 1995.

Bengtsson, L., Andrae, U., Aspelien, T., Batrak, Y., Calvo, J., de Rooy, W., Gleeson, E., Hansen-Sass, B., Homleid, M., Hortal, M., Ivarsson, K.-I., Lenderink, G., Niemelä, S., Nielsen, K. P., Onvlee, J., Rontu, L., Samuelsson, P., Muñoz, D. S., Subias, A., Tijm, S., Toll, V., Yang, X., and Køltzow, M. Ø.: Ø., 2017. The HARMONIE–AROME Model Configuration in the ALADIN–HIRLAM NWP System., Monthly Weather Review, 145, 1919–1935., https://doi.org/10.1175/MWR-D-16-0417.1, 2017.

Björnsson, H.: , 2017. The glaciers of Iceland, Atlantis Press, Amsterdam (Netherlands), 613 pp., 2017. Springer Berlin Heidelberg, Atlantis Press, Amsterdam, Netherlands, 613 p.

Björnsson, H. and Pálsson, F.: Icelandic glaciers, Jökull, 58, 365–386, 2008.
Björnsson, H., Pálsson, F., 2008. Icelandic glaciers. Jökull 58, 365–386.

Björnsson, H. and , Pálsson, F.: , 2020. Radio-echo soundings on Icelandic temperate glaciers: history of techniques and findings., Ann. Glaciol., 1–10., https://doi.org/10.1017/aog.2020.10, 2020.

Björnsson, H., Paálsson, F., Gudmundsson, M. T., and Haraldsson, H. H.: H., 1998. Mass balance of western and northern Vatnajökull, Iceland, 1991-1995., Jökull, 45, 35–38, 1998.

Björnsson, H., Pálsson, F., Gudmundsson, S., Magnússon, E., Adalgeirsdóttir, G., Jóhannesson, T., Berthier, E., Sigurdsson, O., and Thorsteinsson, T.: Contribution of Icelandic ice caps to sea level rise: Trends and variability since the Little Ice Age: MASS LOSS FROM ICELANDIC ICE CAPS, Geophysical Research Letters, 40, 1546–1550, https://doi.org/10.1002/grl.50278, 2013.

Björnsson, H., Pálsson, F., Guðmundsson, S., Magnuson, E., Aðalgeirsdóttir, G., Jóhannesson, T., Berthier, E., Sigurðsson, O., Thorsteinsson, T., 2013. Contribution of Icelandic ice caps to sea level rise: Trends and variability since the Little Ice Age: MASS LOSS FROM ICELANDIC ICE CAPS. Geophysical Res. Lett. 40, 1546–1550. https://doi.org/10.1002/grl.50278

Bogadóttir, H., Boulton, G. S., Tómasson, H., and Thors, K.: , 1986. The structure of the sediments beneath Breiðamerkursandur and the form of the underlying bedrock., in: Iceland Coastal and River Symposium. Proceedings. National Energy Authority, Reykjavík, 295–303, 1986.

Boulton, G. S., Harris, P., and Jarvis, J.: , 1982. Stratigraphy and structure of a coastal sediment wedge of glacial origin inferred from sparker measurements in glacial Lake Jökulsárlón in southeastern Iceland., Jökull, 37–47, 1982.

Bouwer, H. and , Rice, R. C.: C., 1976. A slug test for determining hydraulic conductivity of unconfined aquifers with completely or partially penetrating wells., Water Resour. Res., 12, 423–428., https://doi.org/10.1029/WR012i003p00423, 1976.

Bueler, E., Brown, J., 2009. Shallow shelf approximation as a "sliding law" in a thermomechanically coupled ice sheet model. J. Geophys. Res. 114, F03008. https://doi.org/10.1029/2008JF001179

Burchardt, S., Tanner, D. C., Troll, V. R., Krumbholz, M., and Gustafsson, L. E.: E., 2011. Three-dimensional geometry of concentric intrusive sheet swarms in the Geitafell and the Dyrfjöll volcanoes, eastern Iceland: inclined sheets in Icelandic volcanoes., Geochemistry, Geophysics, Geosystems, 12, n/a-n/a., https://doi.org/10.1029/2011GC003527, 2011.

Cogley, J. G., Hock, R., Rasmussen, L. A., Arendt, A. A., Bauder, A., Kaser, G., Möller, M., Nicholson, L., and Zemp, M.: Glossary of Glacier Mass Balance and Related Terms, Polar Record, 48, 114, https://doi.org/10.1017/S0032247411000805, 2011.

Cooper, R. J., Wadham, J. L., Tranter, M., Hodgkins, R., and Peters, N. E.: Groundwater hydrochemistry in the active layer of the proglacial zone, Finsterwalderbreen, Svalbard, Journal of Hydrology, 269, 208–223, https://doi.org/10.1016/S0022-1694(02)00279-2, 2002.

Crochet, P., Jóhannesson, T., Jónsson, T., Sigurðsson, O., Björnsson, H., Pálsson, F., and Barstad, I.: Estimating the Spatial Distribution of Precipitation in Iceland Using a Linear Model of Orographic Precipitation, Journal of Hydrometeorology, 8, 1285–1306, https://doi.org/10.1175/2007JHM795.1, 2007.

Cogley, J.G., Hock, R., Rasmussen, L.A., Arendt, A.A., Bauder, A., Kaser, G., Möller, M., Nicholson, L., Zemp, M., 2011. Glossary of Glacier Mass Balance and Related Terms. Polar Record 48, 114. https://doi.org/10.1017/S0032247411000805

Cooper, R.J., Wadham, J.L., Tranter, M., Hodgkins, R., Peters, N.E., 2002. Groundwater hydrochemistry in the active layer of the proglacial zone, Finsterwalderbreen, Svalbard. J. of Hydrol. 269, 208–223. https://doi.org/10.1016/S0022-1694(02)00279-2

Crochet, P., Jóhannesson, T., Jónsson, T., Sigurðsson, O., Björnsson, H., Pálsson, F., Barstad, I., 2007. Estimating the Spatial Distribution of Precipitation in Iceland Using a Linear Model of Orographic Precipitation. J. of Hydrometeorology 8, 1285–1306. https://doi.org/10.1175/2007JHM795.1

CropWat 8.0

Crosbie, R. S., Binning, P., and Kalma, J. D.: A time series approach to inferring groundwater recharge using the water table fluctuation method: INFERRING GROUNDWATER RECHARGE, Water Resour. Res., 41, https://doi.org/10.1029/2004WR003077, 2005.

Deuerling, K. M., Martin, J. B., Martin, E. E., and Scribner, C. A.: Hydrologic exchange and chemical weathering in a proglacial watershed near Kangerlussuaq, west Greenland, Journal of Hydrology, 556, 220–232, https://doi.org/10.1016/j.jhydrol.2017.11.002, 2018.

Dochartaigh, B. É. Ó., MacDonald, A. M., Wilson, P., and Bonsor, H. C.: Groundwater investigations at Virkisjökull, Iceland: Data Report 2012, British Geological Survey, 52 pp., 2012.

Dochartaigh, B. É. Ó., MacDonald, A. M., Black, A. R., Everest, J., Wilson, P., Darling, W. G., Jones, L., and Raines, M.: Groundwater–glacier meltwater interaction in proglacial aquifers, Hydrol. Earth Syst. Sci., 23, 4527–4539, https://doi.org/10.5194/hess-23-4527-2019, 2019.

Dochartaigh, B.É.Ó., MacDonald, A.M., Black, A.R., Everest, J., Wilson, P., Darling, W.G., Jones, L., Raines, M., 2019. Groundwater–glacier meltwater interaction in proglacial aquifers. Hydrol. Earth Syst. Sci. 23, 4527–4539. https://doi.org/10.5194/hess-23-4527-2019

Dreimanis, A.: Penecontemporaneous partial disaggregation and/or resedimentation during the formation and deposition of subglacial ti11, Acta Geologica Hispanica, 18, 153–160, 1983.

Einarsson, Þ.: Geology of Iceland: rocks and landscape, Mál og Menning, Reykjavik, 309 pp., 1994.

Deuerling, K.M., Martin, J.B., Martin, E.E., Scribner, C.A., 2018. Hydrologic exchange and chemical weathering in a proglacial watershed near Kangerlussuaq, west Greenland. J. of Hydrol. 556, 220–232. https://doi.org/10.1016/j.jhydrol.2017.11.002

Einarsson, Þ., 1994. Geology of Iceland: rocks and landscape. Mál og Menning, Reykjavik, Iceland, 309p.

Evans, D. J.: J., 2000. A gravel outwash/deformation till continuum, Skaálafellsjoökull, Iceland,. Geografiska. Annaler: Series A, Physical Geography,. 82, 499–512, 2000.

Evans, D. J. A. and J.A., Hiemstra, J. F.: F., 2005. Till deposition by glacier submarginal, incremental thickening,. Earth Surf. Process. Landforms, 30, 1633–1662,. https://doi.org/10.1002/esp.1224, 2005.

Fetter, C. W.: Applied hydrogeology, 4th ed., Prentice Hall, Upper Saddle River, N.J, 598 pp., 2001.

Fetter, C.W., 2001. Applied hydrogeology, 4th ed., ed. Prentice Hall, Upper Saddle River, USA, 598p.

Foundation, T.D., LibreOffice, 2020

Gardner, A.S., Moholdt, G., Cogley, J.G., Wouters, B., Arendt, A.A., Wahr, J., Berthier, E., Hock, R., Pfeffer, W.T., Kaser, G., Ligtenberg, S.R.M., Bolch, T., Sharp, M.J., Hagen, J.O., van den Broeke, M.R., Paul, F., 2013. A Reconciled Estimate of Glacier Contributions to Sea Level Rise: 2003 to 2009. Science 340, 852–857. https://doi.org/10.1126/science.1234532

Goldthwait, R. P. (Ed.): , 1971. Till: a symposium, Ohio State University Press., 414 pp., 1971., USA, 414p.

Guðmundsson, S., Björnsson, H., Pálsson, F., Magnússon, E., Sæmundsson, Þ., and Jóhannesson, T.: Terminus lakes on the south side of Vatnajökull ice cap, SE-Iceland, JOKL, 69, 1–34, https://doi.org/10.33799/jokull2019.69.001, 2020.

Hannesdóttir, H., Zöhrer, A., Davids, H., Sigurgeirsdóttir, S. I., Skírnisdóttir, H., and Árnason, Þ.: Vatnajökull National Park: Geology and Geodynamics, 2010.

Guðmundsson, S., Björnsson, H., Pálsson, F., Magnússon, E., Sæmundsson, Þ., Jóhannesson, T., 2020. Terminus lakes on the south side of Vatnajökull ice cap, SE-Iceland. JOKL 69, 1–34. https://doi.org/10.33799/jokull2019.69.001

Hannesdóttir, H., Zöhrer, A., Davids, H., Sigurgeirsdóttir, S.I., Skírnisdóttir, H., Árnason, Þ., 2010. Vatnajökull National Park: Geology and Geodynamics.

Hannesdóttir, H., Björnsson, H., Pálsson, F., Aðalgeirsdóttir, G., Guðmundsson, S., 2015. Variations of southeast Vatnajökull ice cap (Iceland) 1650-1900 and reconstruction of the glacier surface geometry at the Little Ice Age maximum: Timing and reconstruction of the LIA maximum of SE-Vatnajökull. Geografiska Annaler: Series A, Physical Geography 97, 237–264. https://doi.org/10.1111/geoa.12064

Hannesdóttir, H., Björnsson, H., Pálsson, F., Aðalgeirsdóttir, G., and Guðmundsson, S.: Variations of southeast Vatnajökull ice cap (Iceland) 1650-1900 and reconstruction of the glacier surface geometry at the Little Ice Age maximum: Timing and reconstruction of the LIA maximum of SE-Vatnajökull, Geografiska Annaler: Series A, Physical Geography, 97, 237–264, https://doi.org/10.1111/geoa.12064, 2015.

Hart, J.K., 2017. Subglacial till formation: Microscale processes within the subglacial shear zone. Quaternary Sci. Rev. 170, 26–44. https://doi.org/10.1016/j.quascirev.2017.06.021

Hart, J. K.: Subglacial till formation: Microscale processes within the subglacial shear zone, Quaternary Science Reviews, 170, 26–44, https://doi.org/10.1016/j.quascirev.2017.06.021, 2017.

Hart, J. K., Rose, K. C., Clayton, A., and Martinez, K.: , 2015. Englacial and subglacial water flow at Skálafellsjökull, Iceland derived from ground penetrating radar, in situ Glacsweb probe and borehole water level measurements,. Earth Surface. Processes. and Landforms, 40, 2071–2083,. https://doi.org/10.1002/esp.3783, 2015.

Healy, R. W. and W., Cook, P. G.: G., 2002. Using groundwater levels to estimate recharge,. Hydrogeology Journal,. 10, 91–109,. https://doi.org/10.1007/s10040-001-0178-0, 86 pp., 2002.

Heath, R. C.: C., 1983. Basic ground-water hydrology, . (No. Water-Supply Paper 2220), Water-Supply Paper. U.S. Geological Survey, 1983.

33

Hvorslev~~vorslev~~, M. J.: ~~J., 1951.~~ Time lag and soil permeability in ground-water observations., ~~(No. 36).~~ Corps of Engineers, US Army, Waterways Experiment Station, 1951.

Icelandic Meteorological Office: Icelandic Meteorological Office Database, deliveries no. 2022-07-07/GEJ06, no. 2022-03-30/GEJ02, no. 2022-03-28/GEJ03, Icelandic Meteorological Office, 2022.

Immerzeel, W. W., Lutz, A. F., Andrade, M., Bahl, A., Biemans, H., Bolch, T., & Baillie, J. E. M.: Importance and vulnerability of the world's water towers, Nature, 577(7790), 364-369, https://doi.org/10.1038/s41586-019-1822-y, 2020.

~~Icelandic Meteorological Office 2022: Icelandic Meteorological Office Database, deliveries no. 2022-07-07/GEJ06, no. 2022-03-30/GEJ02, no. 2022-03-28/GEJ03~~

~~IslandsDEMv1, n.d.. Landmælingar Íslands / National Land Survey of Iceland, atlas.lmi.is/dem.~~

Iverson, N. R., McCracken, R. G., Zoet, L. K., Benediktsson, Í. Ö., Schomacker, A., Johnson, M. D., and Woodard, J.: ~~, 2017.~~ A Theoretical Model of Drumlin Formation Based on Observations at Múlajökull, Iceland., J. Geophys. Res. Earth Surf., 122, 2302–2323., https://doi.org/10.1002/2017JF004354, 2017.

Jayne, R. S. and ~~S.,~~ Pollyea, R. M.: ~~M., 2018.~~ Permeability correlation structure of the Columbia River Plateau and implications for fluid system architecture in continental large igneous provinces., Geology, 46, 715–718., https://doi.org/10.1130/G45001.1, 2018.

Jóhannesson, H. and ~~,~~ Sæmundsson, K.: ~~, 1998.~~ Geological Map of Iceland, 1:500 000: Bedrock Geology, Icelandic Institute of Natural History (Náttúrufræðistofnun Íslands), 1998.

Jóhannesson, T., Björnsson, H., Magnússon, E., Guðmundsson, S., Pálsson, F., Sigurðsson, O., Thorsteinsson, T., and Berthier, E.: ~~, 2013.~~ Ice-volume changes, bias estimation of mass-balance measurements and changes in subglacial lakes derived by lidar mapping of the surface of Icelandic glaciers., Ann. Glaciol., 54, 63–74., https://doi.org/10.3189/2013AoG63A422, 2013.

Jóhannesson, T., Pálmason, B., Hjartarson, Á., Jarosch, A. H., Magnússon, E., Belart, J. M. ~~M.~~-C., and Gudmundsson, M. T.: ~~T., 2020.~~ Non-surface mass balance of glaciers in Iceland., J. Glaciol., 1–13., https://doi.org/10.1017/jog.2020.37, 2020.

Join, J.-L.: Caractérisation hydrogéologique du milieu volcanique insulaire : Piton des Neiges, Île de la Réunion, PhD, Université de Montpellier II, 61 pp., 1991.

~~Join, J.L., 1991. Caractérisation hydrogéologique du milieu volcanique insulaire : Piton des Neiges, Île de la Réunion, Ph. D. Thesis, University of Montpellier II~~

Jonsson, B. and ~~,~~ Þorolfur, H.: ~~, 1991.~~ Fljotsdalur Hydroelectric Project ~~(Engineering Geological Report No. OS-91001/VOD-01),~~ Orkustofnun, 90pp., 1991.

Lachassagne, P., Aunay, B., Frissant, N., Guilbert, M., and Malard, A.: ~~, 2014.~~ High-resolution conceptual hydrogeological model of complex basaltic volcanic islands: a Mayotte, Comoros, case study., Terra Nova, 26, 307–321., https://doi.org/10.1111/ter.12102, 2014.

Landmælinga Íslands / National Land Survey of Iceland: IslandsDEMv1, Landmælinga Íslands / National Land Survey of Iceland, n.d.

MacDonald, A. M., Maurice, L., Dobbs, M. R., Reeves, H. J., and Auton, C. A.: Relating in situ hydraulic conductivity, particle size and relative density of superficial deposits in a heterogeneous catchment, Journal of Hydrology, 434–435, 130–141, https://doi.org/10.1016/j.jhydrol.2012.01.018, 2012.

Li, H., Beldring, S., Xu, C.-Y., Huss, M., Melvold, K., Jain, S.K., 2015. Integrating a glacier retreat model into a hydrological model – Case studies of three glacierised catchments in Norway and Himalayan region. Journal of Hydrology 527, 656–667. https://doi.org/10.1016/j.jhydrol.2015.05.017

MacDonald, A.M., Maurice, L., Dobbs, M.R., Reeves, H.J., Auton, C.A., 2012. Relating in situ hydraulic conductivity, particle size and relative density of superficial deposits in a heterogeneous catchment. J. of Hydrol. 434–435, 130–141. https://doi.org/10.1016/j.jhydrol.2012.01.018

Mackay, J. D., Barrand, N. E., Hannah, D. M., Krause, S., Jackson, C. R., Everest, J., MacDonald, A. M., and Ó Dochartaigh, B. É.: Proglacial groundwater storage dynamics under climate change and glacier retreat, Hydrological Processes, hyp.13961, https://doi.org/10.1002/hyp.13961, 2020.

Martin, E., Paquette, J. L., Bosse, V., Ruffet, G., Tiepolo, M., and Sigmarsson, O.: Geodynamics of rift–plume interaction in Iceland as constrained by new 40Ar/39Ar and in situ U–Pb zircon ages, Earth and Planetary Science Letters, 311, 28–38, https://doi.org/10.1016/j.epsl.2011.08.036, 2011.

Monteith, J. L.: Evaporation and environment, Symposia of the Society for Experimental Biology, Cambridge University Press (CUP) 19, 205–234, 1965.

Morris, D. A. and Johnson, A. I.: Summary of hydrologic and physical properties of rock and soil materials as analyzed by the Hydrologic Laboratory of the U.S. Geological Survey, (Water-Supply Paper No. Water-Supply Paper 1839-D). U.S. Geological Survey, 42pp., 1967.

Nawri, N., Pálmason, B., Petersen, N., Björnsson, H., and Þorsteinsson, S.: The ICRA Atmospheric Reanalysis Project for Iceland, (Technical report No. VÍ 2017-005). Icelandic Meteorological Office, 39pp., 2017.

Noël, B., Aðalgeirsdóttir, G., Pálsson, F., Wouters, B., Lhermitte, S., Haacker, J. M., and Broeke, M. R.: North Atlantic Cooling is Slowing Down Mass Loss of Icelandic Glaciers, Geophysical Research Letters, 49, https://doi.org/10.1029/2021GL095697, 2022.

Pálsson, F., Gunnarsson, A., Magnússon, E., Pálsson, H. S., Steinþórsson, S., Hannesdóttir, H., and Þórhallsson, R.: VATNAJÖKULL: Mass balance, meltwater drainage and surface velocity of the glacial year 2020_21, (No. RH-1-2022). Institute of Earth Sciences, University of Iceland and National Power Company, 2022, n.d.

Penman, H. L.: Natural evaporation from open water, bare soil and grass, Proceedings of the Royal Society of London. Series A. Mathematical and Physical Sciences, 193, 120–145, 1948.

Porter, C., Morin, P., Howat, I., Noh, M.-J., Bates, B., Peterman, K., Keesey, S., Schlenk, M., Gardiner, J., Tomko, K., Willis, M., Kelleher, C., Cloutier, M., Husby, E., Foga, S., Nakamura, H., Platson, M., Wethington, M., Williamson, C., Bauer, G., Enos, J., Arnold, G., Kramer, W., Becker, P., Doshi, A., D'Souza, C., Cummens, P., Laurier, F., and Bojesen, M.: ArcticDEM, https://doi.org/10.7910/DVN/OHHUKH, 2018.

QGIS Association: QGIS Geographic Information System, 2022.

Python.org 2022

QGIS.org, 2022

Rhoades, J. D., Kandiah, A., and Mashali, A. M.: The use of saline waters for crop production, Food and Agriculture Organization of the United Nations, Rome, 133 pp., 1992. Italy, 133p.

Robson, S. G.: Techniques for estimating specific yield and specific retention from grain-size data and geophysical logs from clastic bedrock aquifers, (Water Resources Investigations No. 93–4198). US Department of the Interior, US Geological Survey, 1993.

Rounce, D. R., Hock, R., Maussion, F., Hugonnet, R., Kochtitzky, W., Huss, M., & McNabb, R. W.: Global glacier change in the 21st century: Every increase in temperature matters. Science, 379(6627), 78-83, 10.1126/science.abo1324, 2023.

SÆMUNDSSON, K.: , 1979. Outline of the geology of Iceland, Jökull, 29, 7–28, 1979.

Schmidt, L. S., Aðalgeirsdóttir, G., Pálsson, F., Langen, P. L., Guðmundsson, S., and Björnsson, H.: , 2020. Dynamic simulations of Vatnajökull ice cap from 1980 to 2300, J. Glaciol., 66, 97–112, https://doi.org/10.1017/jog.2019.90, 2020.

Sigurðarson, D., Smárason, Ó. B., and Þórðarson, Þ.: , 2016. Hali í Suðursveit Greining jarðlaga í holu HA-25, Baccalaureus Scientiarum, Háskóli Íslands, 61 pp., 2016.

Sigurðsson, F.: Groundwater from glacial areas in Iceland, Jökull, 40, 119–146, 1990.

Sigurðsson, F., 1990. Groundwater from glacial areas in Iceland. Jökull 40, 119–146.

Somers, L.D., Gordon, R.P., McKenzie, J.M., Lautz, L.K., Wigmore, O., Glose, A., Glas, R., Aubry-Wake, C., Mark, B., Baraer, M., Condom, T., 2016. Quantifying groundwater-surface water interactions in a proglacial valley, Cordillera Blanca, Peru: Groundwater Tracing in a Proglacial Catchment. Hydrol. Process. 30, 2915–2929. https://doi.org/10.1002/hyp.10912

Thornthwaite, C. W.: W., 1948. An Approach toward a Rational Classification of Climate, Geographical Review, 38, 55–94, 1948.

Torfason, H.: Investigations into the structure of South-Eastern Iceland, PhD, University of Liverpool, 1979.

Torfason, H., 1979. Investigations into the structure of South-Eastern Iceland, Ph. D. Thesis, University of Liverpool.

Van Vliet-Lanoë, B., Bergerat, F., Geoffroy, L., Guillou, H., and Maury, R. C.: C., 2021. L'Islande au coeur de l'Atlantique Nord, ISTE edition, 258 pp., 2021. London, Great Britain, 258p.

Vincent, A., Violette, S., and Aðalgeirsdóttir, G.: , 2019. Groundwater in catchments headed by temperate glaciers: A review, Earth-Science Reviews, 188, 59–76, https://doi.org/10.1016/j.earscirev.2018.10.017, 2019.

Violette, S., Ledoux, E., Goblet, P., and Carbonnel, J.-P.: , 1997. Hydrologic and thermal modeling of an active volcano: the Piton de la Fournaise, Reunion, Journal J. of Hydrology, 191, 37–63, https://doi.org/10.1016/S0022-1694(96)03071-5, 1997.

World Meteorological Association: State of Global Climate 2021 - WMO, World Meteorological Association, 47pp., 2022.

WMO, 2021,State of Global Climate, WMO Provisional report, 2021. World Meteorological Organization.

Xiang, L., Wang, H., Steffen, H., Wu, P., Jia, L., Jiang, L., and Shen, Q.: , 2016. Groundwater storage changes in the Tibetan Plateau and adjacent areas revealed from GRACE satellite gravity data, Earth and Planetary Science Letters, 449, 228–239, https://doi.org/10.1016/j.epsl.2016.06.002, 2016.

Young, D. S., Hart, J. K., and Martinez, K.: , 2015. Image analysis techniques to estimate river discharge using time-lapse cameras in remote locations, Computers & Geosciences, 76, 1–10, https://doi.org/10.1016/j.cageo.2014.11.008, 2015.